

Electronic Tunnelling Time in Nanostructures

V. Gasparian¹

Department of Physics, California State University, Bakersfield, California, USA

M. Ortuño, O. del Barco

Departamento de Física, Universidad de Murcia, Spain

CONTENTS

1. Introduction
 2. Larmor Clock Approach
 3. Other Approaches
 4. Numerical Results
 5. Conclusions and Outlook
- Glossary
Acknowledgment
References

1. INTRODUCTION

During the last few years key subjects and, consequently, terms in materials research have been continuously changing, indicating a tendency towards smaller and smaller scales. The physics of “low-dimensional structures” was replaced by the discipline of “submicron physics,” emphasizing the effects due to a reduction of size. Then the term “mesoscopic systems” was introduced referring to typical length-scales ranging from a few nanometers up to a few micrometers. Mesoscopic systems are so small, that a complete quantum-mechanical treatment of electrons is required if one wants to describe their transport properties. On the other hand, they are so large, that an exact microscopic description, starting from precise location of impurities and sample boundaries, is not useful, since only the slightest change of the mesoscopic details will completely change the result. More recently still, the terms “nanophase” and “nanostructured materials” have become popular, indicating

that scientists had learned to manipulate, synthesize, analyze, and observe objects approaching the molecular and atomic scales.

Often one distinguishes between “physical” and “chemical nanostructures.” Under the term “physical nanostructures” are classified all artificially built up structures, as obtained, for example, by evaporation and subsequent deposition of materials. On the other hand, the term “chemical nanostructures” comprises all those nanophase materials that can be obtained by methods of chemical synthesis, such as the chemical compounds with chainlike or layer-type structures, as well as the cluster compounds. A review of the electronic properties of nanophase materials obtained from chemical synthesis was given by de Jongh [1]. A survey of chemically synthesized metal clusters was edited by Schmid [2]. The prospect of the applications of metal and semiconductor clusters in inorganic host structures was presented by Simon and Schön [3].

The time spent by a particle in a given region of space is not a new problem, although recently it has attracted a great deal of interest [4–16]. The problem has been approached from many different points of view, and there exists a huge literature on the tunnelling problem of electrons through a barrier, although tunnelling times have continued to be controversial even until now. As pointed out by Landauer and Martin [11], there is no clear consensus about simple expressions for the time in quantum mechanics (QM), where there is not a Hermitian operator associated with it. The problem of the tunnelling time of single electrons (SE) in nanostructures or in mesoscopic systems smaller than 10 nm becomes even more complicated, due to the Coulomb blockade effects [17] on small amounts of electrons and discreteness of electric charge.

In the present review we present the theoretical approaches to tunnelling times to illustrate the problems involved in nanostructures. But this plan proved to be more difficult

¹Also at Department of Physics, Yerevan State University, 375049 Yerevan, Armenia.

than expected: although there exists an extended literature on tunnelling times (see [11] and [4] and references therein), quantum-mechanical treatments mostly deal with propagating wavepackets in a more or less general way and they do not concentrate on tunnelling times in nanostructures. As far as we know, there is not yet a proper treatment about tunnelling times in very small nanostructures with single, localized electrons, where the radius of “localization” is in the same order of magnitude as the length of the barrier L . Thus it proved to be necessary not simply to present the existing models and theories on tunnelling time but to review them with respect to these necessities together with possible alternatives and to estimate future developments. In this context some original works will be analyzed from this point of view. We will be particularly concerned with the closed analytical treatment based on Green’s function formalism.

In the main part of the chapter we study the Larmor clock approach to tunnelling time, based on measuring the spin rotation of an electron under a weak magnetic field acting on the region of interest. We also develop a Green’s function formalism for the traversal, reflection, and dwell times based on the previous approach. The latter corresponds to the amount of time that a particle spends in a region independently of whether it later is transmitted or reflected. We review the rest of the existing major approaches to the time problem in Section 3. In Section 4, we present numerical results about the traversal time in rectangular barriers including finite size effects. We finally extract some conclusions and present open questions.

1.1. Tunnelling Time

Tunnelling refers to the classically impossible process of a particle to penetrate an energy barrier when its energy is smaller than the maximum of the potential of the barrier. The main magnitudes involved in the problem are the height V_0 and the length L of the potential barrier. If they are large, the probability to penetrate the barrier is very small and we say that it is an opaque barrier. Examples of tunnelling processes are α -decay, transmission of electromagnetic waves (EMW) in undersized waveguides, and tunnelling of electrons. A quantum particle usually is said to have an intrinsic “wave nature,” often paraphrased by “wave functions” or “wavepackets.” The probability to penetrate a barrier, which is quantified through the transmission coefficient (probability) T , strongly depends on the nature of the exponential decay of the wave function under the barrier.

Tunnelling of electrons has been of utmost importance for all fast effects in ME. The first device used as a fast switch was the semiconductor tunnel-diode which was commercially introduced in the late 1950s [18]. But again, only its total relaxation time was of interest and not the pure tunnelling time through the bounding barrier. Until relatively recently, little attention was paid to Hartman’s theoretical work on tunnelling time of wavepackets in the 1960s [19]. His main striking result was that under certain circumstances (opaque barrier) the tunnelling time is independent of L and the traversal time can be less than the time that would be required to travel a distance equal to L in vacuum. Similar results were found by Rybachenko [20] for electrons in a rectangular barrier. Although these were excellent pioneer

works, 30 years ago time was not ripe for a further evaluation with respect to practical consequences in ME or even to philosophical ones. Additionally, many physicists hesitated to deal with Hartman’s results since a very fast tunnelling, or a zero tunnelling time, holds a serious consequence: the tunnelling velocity or the average velocity may become higher than the light velocity c . Thus superluminal speed can be expected [21, 22] or measured in some cases like in experiments where electromagnetic waves pass through a barrier [23–27] or through an optical gap [9, 10, 16].

Since SE tunnelling processes could be evaluated in many nanostructures [28–31], it provided a strong motive for advancing nanofabrication technologies and research on tunnelling, which become important even at room temperature, since the operating temperature of single electron devices is directly related to the geometrical size of the electron localization. In SE the discreteness of the electric charge becomes essential and a quantum-mechanical tunnelling of electrons in a system of rather opaque junctions can be much affected by Coulomb interactions. For ME purposes the electron interactions, the barrier height and shape, and thus the tunnelling probability can be varied at will by externally applied voltages or by injected charges.

Usually in QM we can only measure quantities for which we have introduced a Hermitian operator, for example, energy E , momentum p , coordinate y , and so on. For these quantities, expectation values can be calculated and checked experimentally. However, time appears in the standard quantum-mechanical approach only as a parameter and therefore its expectation value is not defined. Since the beginning of QM, people have been aware of the conceptual problem of how to introduce a time operator with an appropriate classical analog, and there have been different theoretical approaches to find a consistent description of this problem [4, 11, 32].

Moreover, according to QM a particle under a barrier, with energy E smaller than V_0 , can only be observed with a strong inelastic influence. If we fix its coordinate with an accuracy of Δy smaller than the length of the barrier L , it necessarily results in a variation of momentum, caused by the measurement, and correspondingly in a change of the kinetic energy of the particle. This change in energy must be greater than the energy difference between the barrier height V_0 and the energy of the particle E [33]. If such a measurement would be carried out by light quanta, then we would have $\hbar\omega \geq V_0 - E$. The latter result demonstrates impressively that it is practically impossible to measure the propagation time from one coordinate (position) to the next under a barrier. This means that in practice one must try to observe the particle outside the barrier, say left or right of the region of interest. For short wavepackets, where the length of the wavepacket approaches the barrier length L , this means “far” left and “far” right.

One can associate the traversal time with the time during which a transmitted particle interacts with the region of interest, as measured by some physical clock which can detect the particle’s presence after leaving the region. For electrons, this approach can utilize the Larmor precession frequency of the spin produced by a weak magnetic field hypothetically acting within the barrier region [20, 34–36]. Similar procedures have been developed for electromagnetic

waves in [37], where was proposed a clock based on the Faraday effect to measure their interaction time in a slab. Another approach is to calculate the traversal time of a particle through a barrier by following the behavior of a wavepacket and determining the delay due to the structure of the region. In this approach one has to be careful with the interpretation of the results, since, for example, an emerging peak is not necessarily related to the incident peak in a causative way [38]. For more discussions on this problem see, for example, [11] and references therein. Martin and Landauer [39] studied the problem of the traversal time of classical evanescent electromagnetic waves by following the behavior of a wavepacket in a waveguide, and Ruiz and co-workers [15, 40] analyzed their behavior in the optical gap of a periodic structure. Japha and Kurizki [41] used the Faraday effect as a quantum clock for evanescent waves and studied its implications on two-photon correlations.

The problem of defining velocities is equally complicated as that of determining the time. One cannot use just one definition for the velocity both inside and outside the barrier at the same time. Usually, for a quantum particle when going from sub-barrier region to above-barrier region, one can do analytical continuation of the wave function. But in the first case there is an exponential decay of the wave function and in the second case we deal with a free propagation of the electron and so a wave function with oscillations. This analytical continuation is not correct for the velocity under the barrier, because one gets an imaginary velocity. So there is no definition of velocity for sub-barrier regions and as a consequence, in the limit of an opaque barrier or in the forbidden gap of a periodic system, there may be observed a “superluminal” speed.

1.2. Wavepacket Approach and Limits

The simplest model which illustrates the tunnelling problem for a quantum particle is a plane wave incident on a one-dimensional (1D) barrier. Part of the plane wave is reflected and part is transmitted. The above plane wave, which represents the electron in our model, is by nature infinitely large in space. The discussion of whether wavepackets with an infinite extension model the wave function of single photons or electrons and of whether they might be interpreted as signals is complicated [4, 11] and important for ME with nanostructures. Therefore it is better to consider a finite wavepacket and to look at its peak evolution in time (see Fig. 1). Thus the phase time is the time which elapses between the peak of the wavepacket entering the barrier and leaving it and can be defined as the energy derivative of the phase:

$$\tau_\varphi = \hbar \frac{d\varphi}{dE} \quad (1)$$

In some cases this time can be easily calculated, but as was mentioned before, it will lead us to Hartman’s effect. We will see (Section 2) that, in general, more than one tunnelling time are involved in the problem: τ_y , τ_z , and the so-called Büttiker-Landauer $\tau^{\text{BL}} = \sqrt{(\tau_y)^2 + (\tau_z)^2}$. Unfortunately this time is not additive in the sense, that when dividing the length of the barrier $L(y)$ arbitrarily into different parts,

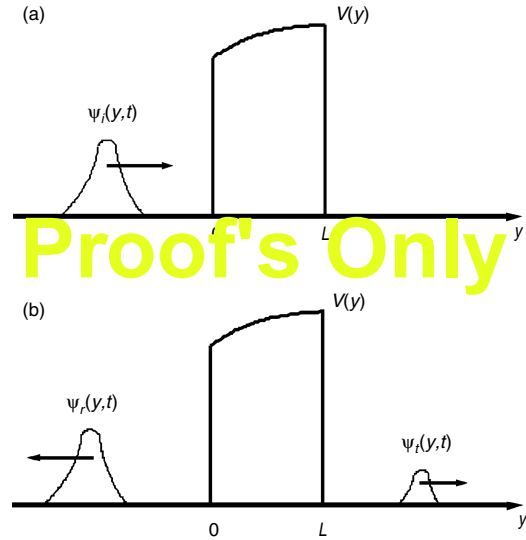


Figure 1. (a) The initial wavepacket enters from the left onto the barrier. (b) Transmitted and reflected wavepackets are moving away from the barrier in opposite directions.

the total τ^{BL} tunnelling time is not the sum of the individual tunnelling times.

To illustrate consequences from the above wavepacket model, let us consider a sharply peaked Gaussian wavepacket in space which starts to enter very far from the barrier to exclude any interaction. A wavepacket is an overlap of many plane waves with different wave numbers k . Hence, one may imagine the wavepacket as something like a group of electrons with different energies and velocities. The propagation will be dispersive and as a consequence the high-energy components of the packet will reach the barrier first. Due to the fact that higher energies can be transmitted more effectively than the low-energy components, the peak of the transmitted packet can leave the barrier long before the peak of the incident packet has arrived [11].

But what is really surprising is that even for the sub-barrier tunnelling, that is, when the wavepacket contains no energy components with energies above the rectangular barrier of height V_0 , the transmitted packet will have a higher mean velocity than the free space propagation velocity. Numerical simulations show that one obtains very short tunnelling times when the spread of the Gaussian wavepacket is larger than the barrier width L . Within these restrictions even the simple rectangular barrier is an “electron accelerator.” This is a manifestation of the aforementioned Hartman effect (see Section 2) which was treated by Rybachenko [20] for spin particles with analogous results. As we will show (Section 2), the tunnelling time component τ_y is independent of L and can be less than the time that would be required for a free particle to travel a distance equal to the barrier thickness L .

As a matter of principle, in ME for high information data rate, the spread of the Gaussian wavepacket must be small. Tunnelling time(s) then will depend to a higher degree on the size of the incident wavepacket and the shape of the barrier: tunnelling will become more sensitive to boundary effects at the barrier.

For the future SE logics in nanostructures, “pure” quantum-mechanical properties of monochromatic single electrons with an energy less than 1 eV will be predominant. For such particles the de Broglie wavelength $\lambda_B = \hbar/p$ will be in the same order of magnitude as the length of the barrier. At the same time, this wavelength will be comparable to the radius of localization (e.g., for electrons confined in the core of ligand-stabilized microclusters) in switches or mass memories (stores). Physically speaking, this means that the picture of a dispersive wavepacket is now failing. As far as we know, fast tunnelling for this case has not been treated theoretically until now.

1.3. Phase Time and Superluminal Velocity in Periodic Nanostructures

In ME the simultaneous transmission of electrons and of microwavepackets of selected optical signals between integrated microchips on wafers is of great importance and today much attention is paid to optoelectronics, since on the way to future ultimate miniaturization, the present generation of devices hopefully will be replaced by nanostructured systems.

While at the end of the preceding section we sketched the problems with localized electrons for the future SE logics in nanostructures, in the present section we first pay attention to microwaves in undersized waveguide barrier-systems and then to photons propagating in 1D periodic and quasi-periodic Fibonacci and Thue-Morse systems. We briefly report about the former first “superluminal” experiment, but we are mainly interested in the latter as there exists a considerable analogy between these periodic systems and, for example, chains of the above chemical nanostructures. So there also must exist forbidden bandgaps where electrons may propagate with “superluminal” speed. It must be noted that periodic structures can be easily built up in crystals of ligand-stabilized microclusters or likewise in chains or layers of supported cluster arrangements on structured wafers or other substrates or even in channels or layer spaces of porous chemical nanostructures (see [3]).

In order to avoid the problems involved with the dispersive nature of the electron’s wavepacket and the invasive measuring process in QM, it was easier to look at a gaussian wavepacket of classical electromagnetic waves and to try to measure the delay time at a barrier. Indeed, in most of the past tunnelling experiments, instead of electrons, electromagnetic waves were used [8, 23], to exclude any electronic interaction with the tunnelling barrier. The analogy between the time-independent forms of the Schrödinger and the Maxwell equations confronts us again with Hartman’s case: the possibility of achieving extremely high tunnelling velocities, even superluminal velocities.

Thus looking back, it was not so surprising that the actual discussion on “superluminal” speed started almost at the same time with the series of microwaves experiments by transmission through systems consisting of undersized waveguides [7, 8, 23–27]. Steinberg et al. [9] found “superluminal” velocities for electromagnetic waves in the photonic bandgap of multilayer dielectric mirrors. Spielman et al. [10] observed that the barrier traversal time of electromagnetic wavepackets tends to become independent of the barrier

thickness for opaque barriers. This phenomenon is closely related to Hartman’s theoretical prediction for electron tunnelling [19]. The theoretical explanation of this phenomenon can be found in the framework of classical Maxwell equations by following the time evolution of the wavepacket in time, as it was mentioned above (see, e.g., [22, 36, 40]). It was clear that parts of the microwavepacket were able to propagate with “superluminal” speed, proving the practical use of Hartman’s effect.

The propagation of electromagnetic waves in 1D quasi-periodic Fibonacci and Thue-Morse systems was studied in [14]. It was shown that, under certain conditions, again the phase time becomes independent of the system size and so “superluminal” group velocities can be obtained for very narrow-frequency-band wavepackets.

2. LARMOR CLOCK APPROACH

Baz’ [34, 35] proposed the use of the Larmor precession to measure the time spent by a spin-1/2 particle inside a sphere of radius $r = a$. He considered the effect of a weak homogeneous magnetic field \mathbf{B} inside the sphere on an incident beam of particles of mass m and kinetic energy $E = \hbar^2 k^2 / 2m$. Let us assume that the magnetic field is directed along the z axis and the incoming particles move along the y axis with their spin polarized along the x axis. As soon as a particle enters the sphere, its magnetic moment will start precessing about the field vector with the well-known Larmor frequency $\omega_L = 2\mu B / \hbar$. The precession will go on as long as the particle remains inside the sphere. The polarization of the transmitted (and reflected) particles is compared with the polarization of the incident particles. The angle θ_\perp in the plane xy , perpendicular to the magnetic field, between the initial and final polarizations is assumed to be given, in the lowest order in the field, by the Larmor frequency ω_L multiplied by the time τ_y spent by the particle in the sphere

$$\theta_\perp = \varphi_L \tau_y \quad (2)$$

The change in polarization thus constitutes a Larmor clock to measure the interaction time of the particles with the region of interest.

Rybachenko [20] considered the simpler problem of the interaction time of particles with a one-dimensional rectangular barrier of height V_0 and width L , for which everything can be calculated analytically. Rybachenko thought that the spin, in first order in the field, remains in the xy plane. For an opaque barrier, where there is a strong exponential decay of the wave function, he found a characteristic interaction time τ_y given by

$$\tau_y = \frac{\hbar k}{V_0 \xi} \quad (3)$$

where ξ is the inverse decay length in the rectangular barrier

$$\xi = (k_0^2 - k^2)^{1/2} \quad (4)$$

with $k_0 = (2mV_0)^{1/2} / \hbar$. This characteristic time τ_y is independent of the barrier thickness L . Instead of being proportional to the length, L is proportional to the decay length.

For an opaque barrier this decay length can become very short and so τ_y can be very small, in fact, smaller than the time that would be required for the incident particle to travel a distance L in the absence of the barrier. A similar result was found by Hartman [19] analyzing the tunnelling of a wavepacket through a rectangular potential barrier, which is known as Hartman's effect.

2.1. Büttiker Approach

Büttiker [36] argued that the main effect of the magnetic field is to tend to align the spin parallel to it in order to minimize the energy. It means that a particle tunnelling through a barrier in a magnetic field does not only perform a Larmor precession, but also a spin rotation produced by the Zeeman effect, which necessarily has to be included in the formalism. The idea behind this Zeeman rotation is the following. A beam of particles polarized in the x direction can be represented as a mixture with equal probabilities of particles with their z component equal to $\hbar/2$ and to $-\hbar/2$. In the barrier the kinetic energy differs by the Zeeman contribution $\pm\hbar\omega_L/2$, giving rise to a different exponential decay of the wave function depending on its spin component along the direction of the magnetic field. In the limit of small fields we have

$$\xi_{\pm} = \left(k_0^2 - k^2 \mp \frac{m\omega_L}{\hbar} \right)^{1/2} \cong \xi \mp \frac{m\omega_L}{2\hbar\xi} \quad (5)$$

where the sign indicates whether the z component of the spin is parallel (+) or antiparallel (−) to the field. The particles with spin $\hbar/2$ will penetrate the barrier more easily than the particles with spin $-\hbar/2$, and so the transmitted particles will have a net z component of the spin. This net component of the spin along the direction of the field defines a second characteristic time τ_z of the particle in the barrier.

For each of the spin components, one can define a characteristic time describing the interaction of the tunnelling particle with the barrier:

$$\lim_{\omega_L \rightarrow 0} \langle S_x \rangle = \frac{\hbar}{2} \left[1 - \frac{\omega_L^2 (\tau_x^{\text{BL}})^2}{2} \right] \quad (6)$$

$$\lim_{\omega_L \rightarrow 0} \langle S_y \rangle = -\frac{\hbar}{2} \omega_L \tau_y^{\text{BL}} \quad (7)$$

$$\lim_{\omega_L \rightarrow 0} \langle S_z \rangle = \frac{\hbar}{2} \omega_L \tau_z^{\text{BL}} \quad (8)$$

Only two of these characteristic times are independent. The spin expectation values $\langle S_x \rangle$, $\langle S_y \rangle$, and $\langle S_z \rangle$ can be obtained in terms of the transmission amplitude for particles with $S_z = \pm\hbar/2$

$$t_{\pm} \equiv \sqrt{T_{\pm}} e^{i\varphi_{\pm}} \quad (9)$$

where T_{\pm} and φ_{\pm} are the corresponding transmission coefficient and phase, respectively.

For the special case of a 1D rectangular barrier, it is possible to find exact analytical expressions for the time. For energies smaller than the height of the barrier, $E < V_0$, Büttiker [36] obtained the following expression for the characteristic time associated with the direction parallel to

the field τ_z^{BL} :

$$\tau_z^{\text{BL}} = -\frac{m}{\hbar\xi} \frac{\partial \ln T^{1/2}}{\partial \xi} \quad (10)$$

For the time τ_y^{BL} associated with the direction of propagation, perpendicular to the field, he found

$$\tau_y^{\text{BL}} = -\frac{m}{\hbar\xi} \frac{\partial \varphi}{\partial \xi} \quad (11)$$

Here T and φ are, respectively, the transmission coefficient (probability) and the phase accumulated by transmitted particles due to the rectangular barrier in the absence of the magnetic field. In Figure 2 we represent τ_y^{BL} and τ_z^{BL} for a rectangular barrier.

Büttiker assumed that the relevant interaction time depends on the times associated to both the Larmor precession and the Zeeman splitting, and is given by

$$\tau^{\text{BL}} = \left\{ (\tau_y^{\text{BL}})^2 + (\tau_z^{\text{BL}})^2 \right\}^{1/2} \quad (12)$$

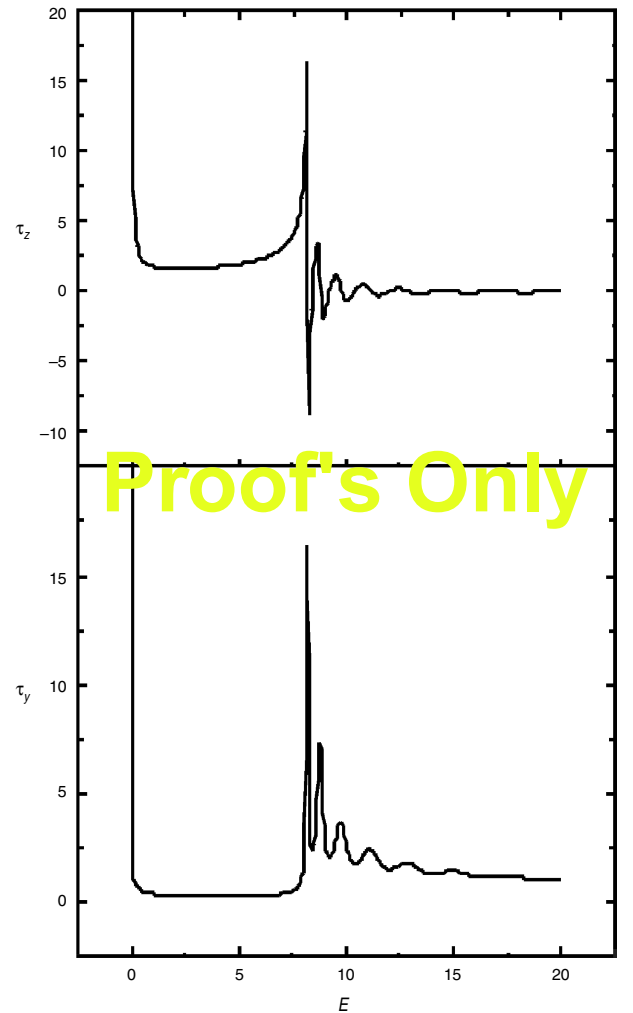


Figure 2. Components τ_y^{BL} and τ_z^{BL} of the Büttiker-Landauer time for a rectangular barrier. For energies higher than the barrier potential, both components oscillate with energy.

This traversal time is the so-called Büttiker-Landauer (BL) time for transmitted particles. Although it was obtained in the context of tunnelling, it is a general definition which applies for the traversal time of a particle or an electromagnetic wave through any given region of space. For a rectangular barrier, it is then given by

$$\tau^{\text{BL}} = \frac{m}{\hbar\xi} \left\{ \left(\frac{\partial \ln T^{1/2}}{\partial \xi} \right)^2 + \left(\frac{\partial \varphi}{\partial \xi} \right)^2 \right\}^{1/2} \quad (13)$$

When the energy E of an incident particle is well below the barrier height V_0 of an opaque rectangular barrier, Büttiker's result (13) is approximately equal to

$$\tau^{\text{BL}} \simeq \frac{mL}{\hbar\xi} \quad (14)$$

which is very different from the result of Rybachenko, Eq. (3). It is, however, in agreement with the traversal time obtained by Büttiker and Landauer [42] based on the transition from adiabatic to sudden limits for a time-modulated rectangular opaque barrier.

2.2. Green's Functions Method

We now derive a general expression for the traversal time using the Green's Function (GF) method [43, 44]. We will consider a 1D system with an arbitrary potential $V(y)$ confined to a finite segment $0 < y < L$, which we will call "the barrier." As for a rectangular barrier, we apply a weak magnetic field \mathbf{B} in the z direction and confined to the barrier (see Fig. 3).

Our electron is incident on the barrier from the left with an energy E and with its spin polarized along the x direction. In the presence of the magnetic field, the Schrödinger equation takes the form

$$\left(-\frac{\hbar^2}{2m} \frac{d^2}{dy^2} + V(y) - E \right) \widehat{\Psi}(y) = -\mu B \begin{pmatrix} 1 & 0 \\ 0 & -1 \end{pmatrix} \widehat{\Psi}(y) \quad (15)$$

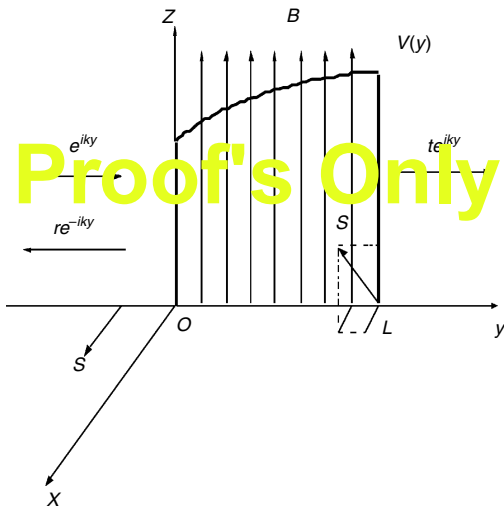


Figure 3. General potential barrier restricted to the interval $0 < y < L$ with a magnetic field applied.

where the column wavevector $\widehat{\Psi}(y)$ represents compactly both spin states.

The problem is solved by perturbation theory. In the lowest order in B , the spinor $\widehat{\Psi}(L)$ of the electron on the right end of the barrier is given by [43]

$$\widehat{\Psi}(L) = \begin{pmatrix} 1 \\ 1 \end{pmatrix} \psi(L) + \frac{e\hbar B}{2mc} \begin{pmatrix} 1 \\ -1 \end{pmatrix} \int_0^L \psi(y) G(y, L) dy \quad (16)$$

Here $\psi(y)$ is the solution of the spatial part of the Schrödinger equation in the absence of the magnetic field, which can be written in terms of the GF of the system as

$$\psi(y) = \exp(iky) - \int_0^L G(y, y') V(y') \exp(iky') dy' \quad (17)$$

where $G(y, y')$ is the retarded GF, whose energy dependence is not written explicitly. It should satisfy Dyson's equation:

$$G(y, y') = G_0(y, y') + \int_0^L G_0(y, y'') V(y'') G(y'', y') dy'' \quad (18)$$

where $G_0(y, y') = i(m/k\hbar^2) \exp(ik|y - y'|)$ is the free-electron GF. We can obtain all the relevant properties of the problem in terms of the GF, solution of the previous equation.

We first concentrate on the calculation of the traversal time. The expectation value of the component of the spin along the direction of the magnetic field of the transmitted electron is, up to second order in B :

$$\begin{aligned} \langle S_z \rangle &= \frac{\hbar}{2} \langle \widehat{\Psi}(L) | \sigma_z | \widehat{\Psi}(L) \rangle \\ &= -\frac{e\hbar^2 B}{mc} \text{Re} \left[\psi^*(L) \int_0^L \psi(y) G(L, y) dy \right] \end{aligned} \quad (19)$$

We want to express the wave function $\psi(y)$ appearing inside the integral in the previous equation in terms of the GF. In order to do so, we take into account the following relationship between the wave function and the GF of a 1D system:

$$\psi(y) = -\frac{i\hbar^2 k}{m} G(0, y) \quad (20)$$

For one-dimensional systems also, we can further simplify the problem by writing the general expression of the GF, $G(y, y')$, in terms of its own expression at coinciding coordinates $y = y'$ [45]. One finds that the spin component along the direction of the magnetic field is given by

$$\langle S_z \rangle = \frac{e\hbar^2 B}{mc} |\psi(L)|^2 \text{Re} \int_0^L G(y, y) dy \quad (21)$$

Similarly, the spin component along the y direction is equal to

$$\langle S_y \rangle = -\frac{e\hbar^2 B}{mc} |\psi(L)|^2 \text{Im} \int_0^L G(y, y) dy \quad (22)$$

Büttiker-Landauer characteristic traversal times for the z and y directions are proportional to the corresponding spin components, Eqs. (8) and (7), and we finally arrive at

$$\tau^{\text{BL}} = \hbar \left| \int_0^L G(y, y) dy \right| \quad (23)$$

Instead of defining the modulus of τ_z^{BL} and τ_y^{BL} as the central magnitude of the problem, we prefer to define a complex traversal time τ as

$$\tau = \tau_z^{\text{BL}} + i\tau_y^{\text{BL}} = \hbar \int_0^L G(y, y) dy \quad (24)$$

As we will see, other approaches also get a complex time. The two characteristic times of the problem can be written in a compact form as the real and imaginary parts of a single well-defined magnitude. Besides, these two time components may be separately relevant to different experimental results, and do not have to necessarily enter into the problem through the modulus, Eq. (23). We will come back to this question.

The final result, Eq. (24), only depends on the integral of the GF at coinciding coordinates. For practical purposes and in order to compare this result with those of other approaches, it is interesting to rewrite it in terms of the transmission t and reflection from the left r and from the right r' amplitudes [44, 45]. The spatial integral, over the length of the barrier, of the GF at coinciding coordinates can be expressed in terms of partial derivatives with respect to energy E :

$$\tau = \hbar \int_0^L G(y, y) dy = \hbar \left\{ \frac{\partial \ln t}{\partial E} + \frac{1}{4E}(r + r') \right\} \quad (25)$$

This is a general expression, independent of the model considered.

The first term in the RHS of Eq. (25) mainly contains information about the region of the barrier. Most of the information about the boundary is provided by the term including the reflection amplitudes r and r' . This term is on the order of the wavelength λ over the length of the system L , and it becomes important for low energies and/or short systems. It can be neglected in the semiclassical WKB case and when r is negligible, for example, in the resonant case, when the influence of the boundaries is negligible. Certain approaches only obtain the contribution to the time proportional to an energy derivative, missing the terms proportional to the reflection amplitudes. The same type of problem arises when calculating densities of states or partial densities of states [46].

The components of the traversal time can be related to the density of states and the resistance. The imaginary part of $G(y, y)$ is proportional to the local density of states at the corresponding energy. So, τ_y^{BL} can also be written as $\tau_y^{\text{BL}} = \pi \hbar L \nu_L(E)$, where $\nu_L(E)$ is the average density of states per unit energy and per unit length.

Thouless has shown [47] the existence of a dispersion relation between the localization length and the density of states. This relationship can be expressed [48] in the form of a linear dispersion relation between the real part, $\text{Re} \ln t$,

and the imaginary part, $\text{Im} \ln t$, of the transmission amplitude. The self-averaging property of τ_z^{BL} and of τ_y^{BL} is therefore an immediate consequence of self-averaging of the localization length and of the density of states [48]. While τ_z and τ_y are additive, the total tunnelling time τ^{BL} , given by Eq. (23), is not the sum of the individual transmission times. This property has also been pointed out by Leavens and Aers [49]. It is a consequence of the fact that, for an infinitesimal B , the interference between the effects of the magnetic field in the separate regions $[0; y]$ and $[y; L]$ is of higher order than linear and does not contribute to the local times [49]. Mathematically speaking, we say that the BL time, Eq. (23), adds as the absolute value of complex additive numbers, and so it is not additive.

2.3. Reflection Time

For reflected particles we can proceed in the same way as we did for transmitted particles. We will use the subindex R to indicate that the magnitude corresponds to reflection, and we understand that similar magnitudes related to transmission will have no subindex. Proceeding as above, we find for the expectation values of the spin components of the reflected wave: and

$$\begin{aligned} \langle S_z \rangle_{\text{R}} &= \frac{\hbar}{2} \langle (\hat{\Psi}(0) - 1) | \sigma_z | (\hat{\Psi}(0) - 1) \rangle \\ &= \frac{e\hbar^2 B}{mc} |\psi^*(0) - 1|^2 \text{Re} \int_0^L \psi(y) G(0, y) dy \end{aligned} \quad (26)$$

and

$$\langle S_y \rangle_{\text{R}} = -\frac{e\hbar^2 B}{mc} |\psi^*(0) - 1|^2 \text{Im} \int_0^L \psi(y) G(0, y) dy \quad (27)$$

We can again define three new characteristic times, $\tau_{z, \text{R}}^{\text{BL}}$, $\tau_{y, \text{R}}^{\text{BL}}$, and $\tau_{x, \text{R}}^{\text{BL}}$, each of them associated with a component of the spin. Only two of these times are independent. Invoking Eqs. (26) and (27) and the relationship (20) between the wave function and the GF of a one-dimensional system, we arrive at

$$\tau_{y, \text{R}}^{\text{BL}} = \hbar \text{Im} \frac{1+r}{r} e^{-i2\theta(0)} \int_0^L G(y, y) e^{i2\theta(y)} dy \quad (28)$$

$$\tau_{z, \text{R}}^{\text{BL}} = \hbar \text{Re} \frac{1+r}{r} e^{-i2\theta(0)} \int_0^L G(y, y) e^{i2\theta(y)} dy \quad (29)$$

where $\theta(y)$ is a phase function given by

$$\theta(y) = \int_0^y \frac{im}{\hbar^2} \frac{dy'}{G(y', y')} \quad (30)$$

The characteristic times $\tau_{y, \text{R}}^{\text{BL}}$ and $\tau_{z, \text{R}}^{\text{BL}}$ are the real and imaginary components, respectively, of a complex quantity. This quantity is proportional to a new integral of the GF at coinciding coordinates, which in this case involves the phase function also. The previous integral can be written in terms of the transmission and reflection amplitudes. We arrive at the following expression for the complex reflection time [50]:

$$\tau_{\text{R}} = \tau_{z, \text{R}}^{\text{BL}} + i\tau_{y, \text{R}}^{\text{BL}} \equiv \hbar \left\{ \frac{\partial \ln r}{\partial E} - \frac{1}{4Er} (1 - r^2 - t^2) \right\} \quad (31)$$

This is again a general equation, independent of the model used.

For an arbitrary symmetric potential, $V((L/2) + y) = V((L/2) - y)$, the total phases accumulated in a transmission and in a reflection event are the same, as can be deduced from the form of the scattering matrix elements, and so the characteristic times for transmission and reflection corresponding to the direction of propagation are equal:

$$\tau_y^{\text{BL}} = \tau_{y,\text{R}}^{\text{BL}} \quad (32)$$

as it immediately follows from Eqs. (25) and (31) (see also the review article by Hauge and Støvneng [4]). For the special case of a rectangular barrier, Eq. (32) was first found by Büttiker [36]. For an asymmetric barrier, Eq. (32) breaks down as discussed by Leavens and Aers [51].

2.4. Dwell Time

There is also another important characteristic time called the dwell time, about which there exists a vast literature (see, e.g., [4, 11] and references therein). This time was first introduced by Büttiker [36] region divided by the average number entering (or leaving) the barrier per unit time. It corresponds to the average time spent by a particle within the barrier irrespective of whether it is finally reflected or transmitted.

The dwell time in a neighborhood of y is defined as the ratio between the particle number in the interval $[y, y + dy]$ and the incoming current [36]:

$$d\tau^{(\text{D})}(y) = \frac{|\psi(y)|^2}{J} dy \quad (33)$$

where $\psi(y)$ is the steady-state scattering solution of the time-independent Schrödinger equation. Obviously, Eq. (33) describes a balance equation: in the stationary case the injected current equals the decay rate of the probability in $[y, y + dy]$. The dwell time $\tau^{(\text{D})}$ of a finite region within the context of a stationary-state scattering problem is obtained via a spatial integration of Eq. (33). So the dwell time $\tau^{(\text{D})}$ is given by [36]

$$\tau^{(\text{D})} \equiv \frac{m}{\hbar k} \int_0^L |\psi(y)|^2 dy \quad (34)$$

Here the integral extends over the barrier, and $\hbar k/m$ is the incident flux. Again we want to calculate this time in terms of the transmission and reflection amplitudes.

Let us consider again a particle moving along the y direction in the presence of an arbitrary potential barrier $V(y)$ in the interval $[0, L]$. Taking explicitly into account that the wave function appearing in Eq. (34) is a solution of the Schrödinger equation, we arrive at [52]

$$\begin{aligned} \tau^{(\text{D})} = & -\frac{\hbar}{4k} \left[\psi^{*2}(y) \frac{\partial}{\partial E} \left(\frac{\psi'(y)\psi(y)}{|\psi(y)|^2} \right) \right. \\ & \left. + \psi^2(y) \frac{\partial}{\partial E} \left(\frac{\psi'^*(y)\psi^*(y)}{|\psi(y)|^2} \right) \right]_0^L \quad (35) \end{aligned}$$

This expression is formally the same for particles incident from the left or from the right, but we have to remember

that the corresponding wave functions will not be the same. García-Calderón and Rubio [53] arrived at the same result by a completely different method.

We can now rewrite Eq. (35) in terms of the retarded GF $G(y, y')$ of the system, as we have been doing for the other times. The dwell time is given by

$$\tau^{(\text{D})} = \left[i \frac{\partial}{\partial E} \theta(y) - G(y, y) \frac{\partial}{\partial E} \left(\frac{G'(y, y)}{G(y, y)} \right) \right]_0^L \quad (36)$$

As it occurs for the wave function, the GF $G(y, y')$ depends on whether the particle arrives to the barrier from the left or from the right. After some cumbersome algebra, we can express the dwell time in terms of the transmission and reflection amplitudes:

$$\begin{aligned} \tau_{-}^{(\text{D})} = & \hbar \text{Im} \left\{ \left[\frac{\partial \ln t}{\partial E} + \frac{1}{4E} (r + r') \right] \right. \\ & \left. + \frac{1}{2} \left[\sqrt{R} \frac{\partial}{\partial E} \ln \frac{r}{r'} + \frac{1}{2E} (r - r') \right] \right\} \quad (37) \end{aligned}$$

The subindex indicates that the particle is coming from the left. R is the modulus square of the reflection amplitudes $R = |r|^2 = |r'|^2$. When the particle is coming from the right, the dwell time is given by an expression similar to Eq. (37), but interchanging r and r' . We will refer to this case with the subindex $+$.

Gasparian et al. [44] showed that the first term on the RHS of Eq. (37) is proportional to the density of states. Then, we finally arrive at the following expression for the dwell time:

$$\tau_{\pm}^{(\text{D})} = \pi \hbar L \nu(E) \pm \frac{\hbar}{2} \text{Im} \left[\sqrt{R} \frac{\partial}{\partial E} \ln \frac{r}{r'} + \frac{1}{2E} (r - r') \right] \quad (38)$$

For a symmetric potential we have that the reflection coefficients from the right and from the left are equal, $r = r'$, and we obtain $\tau_{-}^{(\text{D})} = \tau_{+}^{(\text{D})} = \pi \hbar L \nu(E)$, in agreement with the result of Gasparian and Pollak [43].

For an asymmetric barrier, it is easy to check that the contribution from the asymmetry is the opposite for particles coming from the left and from the right. Then we find that

$$\nu(E) = \frac{1}{2\pi \hbar L} (\tau_{-}^{(\text{D})} + \tau_{+}^{(\text{D})}) \quad (39)$$

This result was obtained in a much wider context by Iannaccone [54], which considered the relation between the dwell time and the density of states for a three-dimensional region Ω of arbitrary shape with an arbitrary number of incoming channels. He arrived at

$$\nu_{\Omega}(E) = \frac{1}{2\pi \hbar} \sum_{n=1}^N \tau_n^{(\text{D})} \quad (40)$$

where $\nu_{\Omega}(E)$ is the density of states per unit volume, and $\tau_n^{(\text{D})}$ is the dwell time for particles coming from the n -channel. This result shows that the density of states in Ω is proportional to the sum of the dwell times in Ω for all the incoming channels.

A controversial question concerning the dwell time is whether it satisfies or not the relation (see [49, 55, 56])

$$\tau^{(D)} = R\tau_{y,R}^{\text{BL}} + T\tau_y^{\text{BL}} \quad (41)$$

This result is trivial for classical particles, for which the traversal time coincides with the y component of our complex traversal time and for which there is no interference between the reflected and the transmitted particles. For the quantum coherent case, this result is not so clear. We can prove this relation, which we believe must hold because a particle incident on the barrier is either transmitted or reflected. Reflection and transmission of a particle are mutually exclusive events in the sense of Feynman and Hibbs [57]; that is, a measurement can determine, without interfering with the scattering event, whether a particle has been transmitted or reflected. Our results for the y component of the transmission and reflection times, Eqs. (25) and (31), respectively, and for the dwell time, Eq. (37), allow us to prove exactly the previous relation between these times. On the other hand, our results also prove that a similar relation involving the full BL times does not hold. This relation has been claimed very often in the literature, and has been strongly criticized by other authors [11].

3. OTHER APPROACHES

In this section, we review other approaches to the problem of the traversal and reflection times. We would like to show that most results, obtained from very different points of view, are almost compatible and coincide with Eq. (25) for the traversal time and with Eq. (31) for the reflection time. Often, these approaches only obtain the contributions to the time proportional to the energy derivative of the logarithm of the transmission amplitude.

We start with the oscillatory incident amplitude and with the time-modulated barrier approaches. Then we review the Feynman path-integral approach, where the idea of a complex time arises more naturally. We finish with the kinetic approach, which is very convenient to study finite size effects and so the standard errors inherent to the problem.

3.1. Oscillatory Incident Amplitude

We assume an incident wave of oscillatory amplitude interacting with a time-independent potential, and study the shape distortion of the transmitted wave by the barrier. This method was proposed by Büttiker and Landauer [58, 59] and analyzed by Leavens and Aers [51] and Martin and Landauer [60]. The incident wave consists of two interfering plane waves:

$$\begin{aligned} \Psi(y, t) &= \exp\left\{i\left[ky - \frac{Et}{\hbar}\right]\right\} \\ &+ \exp\left\{i\left[(k + \Delta k)y - \frac{(E + \Delta E)t}{\hbar}\right]\right\} \\ &= 2 \exp\left\{i\left[(k + \Delta k/2)y - \frac{(E + \Delta E/2)t}{\hbar}\right]\right\} \\ &\times \cos\left(\frac{\Delta ky}{2} - \frac{\Delta Et}{2\hbar}\right) \end{aligned} \quad (42)$$

The energy difference between the two plane waves characterizes the oscillations in amplitude of the incident wave. In the region to the right of the barrier, we have the sum of two transmitted plane waves which can be written in the form

$$\begin{aligned} \Psi(y, t) &= t(E) \left\{ i \left[ky - \frac{Et}{\hbar} \right] \right\} + t(E + \Delta E) \\ &\times \exp\left\{ i \left[(k + \Delta k)y - \frac{(E + \Delta E)t}{\hbar} \right] \right\} \end{aligned} \quad (43)$$

The shape distortion produced by the barrier on the transmitted wave will strongly depend on ΔE . If ΔE is small, the incident wave is modulated very slowly and in that case the transmitted wave (43) will reproduce the incident wave (42), in the sense that the destructive and constructive interferences will occur at the same time for both of them. As we increase ΔE , $t(E)$ and $t(E + \Delta E)$ will increasingly differ and the transmitted wave (43) will no longer reproduce the incident wave. We can assume that appreciable shape distortion will take place when a characteristic time delay, or dispersion in transit time, becomes comparable to or larger than the modulation period [58, 59]. Thus we define a new traversal time τ as $\hbar/\Delta E$, where ΔE is the energy difference which establishes the onset of significant distortion of the transmitted wave, that is, the energy such that $\Delta E |d\alpha(E)/dE| \approx 1$.

The analysis of this approach based on the WKB approximation led Büttiker and Landauer [58] to the following results. For $E < V(y)$, the phase of the transmission amplitude is of secondary importance as compared with the exponential decay of the modulus of $t(E)$. We can write the transmission amplitude in the form

$$t_{\text{WKB}}(E) = \exp\left[-\int_{y_1}^{y_2} \xi(y) dy\right] \quad (44)$$

where ξ is the inverse decay length, given by Eq. (4), and y_1 and y_2 are the classical turning points. From this expression of the transmission amplitude, Büttiker and Landauer obtained for the traversal time for tunnelling

$$\tau_{\text{WKB}}(E) = \frac{m}{\hbar} \left[-\int_{y_1}^{y_2} \frac{dy}{\xi(y)} \right] \quad (45)$$

When $E > V(y)$, the energy dependence of $t(E)$ comes primarily from the dependence of the phase ($|t(E)| = 1$), and then we can assume that $t(E)$ is of the form

$$t_{\text{WKB}}(E) = \exp\left[-i \int_0^L K(y) dy\right] \quad (46)$$

with $K(y) = i\xi(y)$. For this case, in which the phase dominates, we have

$$\tau_{\text{WKB}}(E) = \frac{m}{\hbar} \left[\int_0^L \frac{dy}{K(y)} \right] \quad (47)$$

It is easy to check that, for a rectangular barrier, the traversal time τ_{WKB} is equal to $mL/\hbar\xi$ for energies below the barrier height and equal to $mL/\hbar K$ for energies above the barrier. As it was shown by Martin and Landauer [60], the general analysis of this two-interfering-incident-waves

approach yields characteristic times that depend on energy derivatives of the transmission coefficient

$$\tau = \hbar |t_E^{-1}| \left| \frac{dt_E}{dE} \right| = \hbar \left\{ \left(\frac{d\varphi}{dE} \right)^2 + \left(\frac{d \ln T}{dE} \right)^2 \right\}^{1/2} \quad (48)$$

As in the Büttiker and Landauer approach to the Larmor clock, the time is equal to the square root of the sum of the squares of two characteristic times, one involving energy derivatives of the phase and the other energy derivatives of the logarithm of the modulus of the transmission amplitude. The same result for the traversal time is also obtained in the modulated barrier approach [60].

It is interesting to note that this oscillatory amplitude approach without resort to the WKB approximation led Leavens and Aers [51] to complex times. Let us write the transmission amplitude as

$$t(E) = \exp[i\beta(E)] \quad (49)$$

where $\beta(E)$ is in general complex. For sufficiently small ΔE , we may expand $t(E + \Delta E)$ to lowest order in ΔE :

$$\begin{aligned} t(E + \Delta E) &\cong \exp \left[i \left(\beta(E) + \Delta E \frac{d\beta(E)}{dE} \right) \right] \\ &= t(E) \exp \left[i \Delta E \frac{d\beta(E)}{dE} \right] \end{aligned} \quad (50)$$

This expression should be substituted in Eq. (43) for the transmitted packet. For sufficiently small ΔE , the difference in exponents of the two components of the transmitted wave at $y = L$ and $t = \Delta t$ is greater than that of the two components of the incident wave at $y = 0$ and $t = 0$ by an amount

$$\begin{aligned} &i \left[\Delta k L - \frac{\Delta E}{\hbar \Delta k} \left(\Delta t - \hbar \frac{d\beta(E)}{dE} \right) \right] \\ &\cong i \Delta k \left[L - v(k) \left(\Delta t - \hbar \frac{d\beta(E)}{dE} \right) \right] \end{aligned} \quad (51)$$

with $v(k) \equiv \hbar^{-1} dE/dk = \hbar k/m$ being the group velocity. In the absence of the potential barrier, the traversal time associated with the propagation of the wavepacket from $y = 0$ to $y = L$ is the value of Δt for which $L - v(k)\Delta t = 0$, that is, $\tau = L/v(k)$. Formally, in the presence of the potential, Leavens and Aers [51] obtained from Eq. (51) the complex barrier interaction ‘‘time’’

$$\tau^E = \frac{L}{v(k)} + \hbar \frac{d\beta(E)}{dE} \equiv -i\hbar \frac{\partial \ln t}{\partial E} \quad (52)$$

This final answer for the time is just proportional to $\partial \ln t / \partial E$, and so is correct for infinitely large systems only ($L \gg \lambda$). The difference between this expression for the traversal time and our general expression (25) is the term proportional to the reflection amplitude, which cannot be obtained with this type of approach.

We can deduce explicit expressions for all these times, and so see clearly the difference between Eq. (52) and Eq. (25), obtained with the GF formalism, for the special case of a rectangular barrier. Let us associate the real and imaginary components of this complex time, Eq. (52), with the previous

characteristic times for the y and z components, and let us denote them as τ_y^E and τ_z^E . The explicit expressions for the two components of the traversal time τ_y^E and τ_z^E for this special case of a constant potential can be written in the form [51]

$$\begin{aligned} \tau_z^E &= -\hbar \frac{\partial \ln T^{1/2}}{\partial E} \\ &= \frac{mk_0^4}{2\hbar\xi^2k^2} \frac{2(\xi^2 - k^2)\sinh^2(\xi L) + k^2\xi L \sinh(2\xi L)}{4k^2\xi^2 + k_0^2 \sinh^2(\xi L)} \end{aligned} \quad (53)$$

$$\tau_y^E = \hbar \frac{\partial \varphi}{\partial E} = \frac{m}{\hbar k \xi} \frac{2\xi L k^2 (\xi^2 - k^2) + k_0^4 \sinh(2\xi L)}{4k^2 \xi^2 + k_0^2 \sinh^2(\xi L)} \quad (54)$$

After an obvious change of notation, it is easy to check that the times τ_y^E and τ_z^E are related to the exact results τ_y^{BL} and τ_z^{BL} through

$$\begin{aligned} \tau_y^E &= \tau_y^{\text{BL}} + \frac{1}{2E} \text{Im } r \\ -\tau_z^E &= \tau_z^{\text{BL}} + \frac{1}{2E} \text{Re } r \end{aligned} \quad (55)$$

where τ_z^{BL} and τ_y^{BL} are given by Eqs. (10) and (11). Figure 4 compares τ_y^E with τ_y^{BL} for a rectangular barrier. It can be

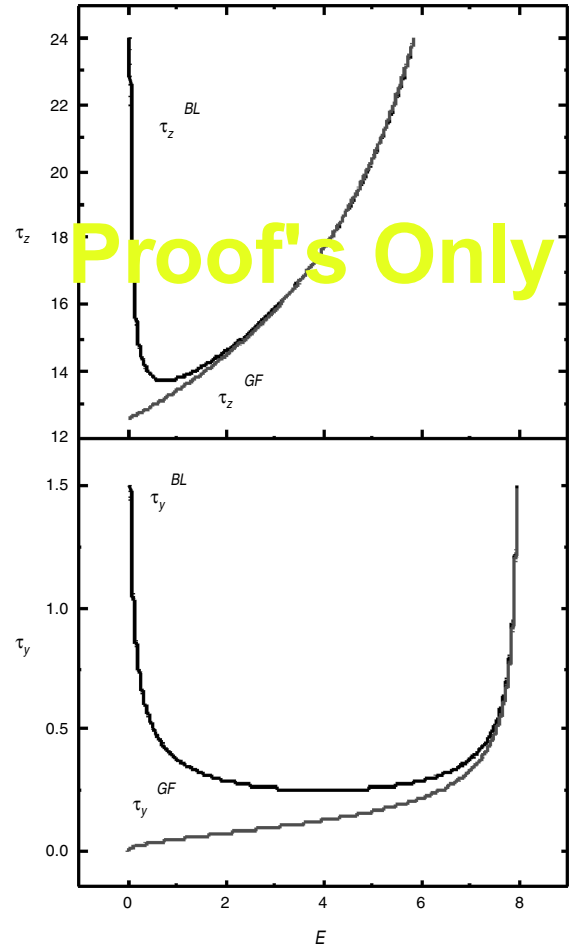


Figure 4. Components of the traversal time for a rectangular barrier according to Eqs. (25) and (54).

seen that, even for an opaque barrier ($\xi L \gg 1$), the differences between these times can be very significant. This is particularly so at very small energy E where τ_y^{BL} goes to zero as $E^{1/2}$, while τ_y^{E} diverges as $E^{-1/2}$, and, at the same time, τ_z^{BL} is approximately equal to 0, while τ_z^{E} diverges as E^{-1} . The oscillatory amplitude approach in general does not give the same answer as the GF formalism, based on the Larmor clock approach. As the difference between the corresponding tunnelling times is proportional to the amplitude of reflection, we concluded that it arises from boundary effects [44].

3.2. Time-Modulated Barrier

The time-modulated barrier approach to the traversal time was introduced by Büttiker and Landauer [42] (see also [58, 61]). Its basic idea is simple and can be explained as follows. Let us add to the static barrier potential which we discussed before a time-dependent potential which is zero everywhere except in the region of interest. So the 1D potential can now be written in the form

$$V(y, t) = V(y) + V_1 \cos(\omega t) \quad (56)$$

where V_1 is the amplitude of the small modulation added, and ω is its corresponding frequency. For the sake of simplicity, it is more convenient in this approach to consider the barrier restricted to the region $-L/2 < y < L/2$.

Suppose that there is a characteristic time τ during which the particle interacts with the barrier. If the period of the modulation $T = 2\pi/\omega$ is long compared to the time τ , then the particle sees an effectively static barrier during its traversal. In the opposite extreme, that is, for slowly tunnelling electrons, for which $\omega\tau > 1$, the barrier oscillates many times during the period of traversal of the electron. There is thus a crossover from a low-frequency behavior to a high-frequency behavior, and we expect to occur two distinct types of electron-barrier interactions, depending on the value of $\omega\tau$ as compared with unity.

We will use a rectangular barrier extensively, for illustrative purposes, but in principle all the results can be generalized to an arbitrary potential barrier by considering the adiabatic limit, $\omega \rightarrow 0$, of this inelastic scattering process [62]. The Hamiltonian for the time-modulated rectangular barrier in the scattering region is

$$H = -\frac{\hbar}{2m} \frac{d^2}{dy^2} + V_0 + V_1 \cos(\omega t) \equiv H_0 + V_1 \cos(\omega t) \quad (57)$$

As it is well known from the time-dependent perturbation theory [63], incident particles with energy E , interacting with the perturbation $V_1 \cos(\omega t)$, will emit or absorb modulation quanta $\hbar\omega$. In first-order corrections to the time-independent case, this means that inside the barrier, for $|y| > L/2$, the reflected and transmitted waves, used to represent the tunnelling electrons, we will now have a main feature at the initial energy E and also sidebands at the energies $E + \hbar\omega$ and $E - \hbar\omega$, as it is schematically represented in Figure 5. Taking V_1 as a perturbation, the two independent eigensolutions of the corresponding

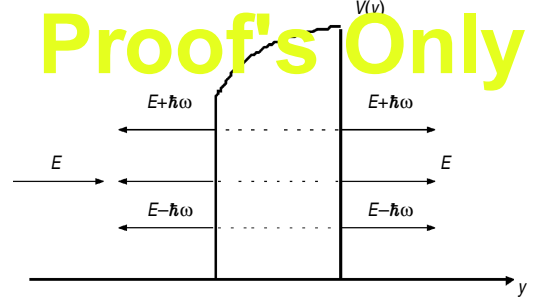


Figure 5. For an oscillating barrier, besides a main transmission and reflection component at the initial energy E , there are two lateral components at energies $E \pm \hbar\omega$. Reprinted with permission from [86], V. Gasparian et al., “Handbook of Nanostructured Materials and Nanotechnology” (H. S. Nalwa, Ed.), Vol. 2, Chapter 11, 1999. © 1999, Elsevier Science.

time-dependent Schrödinger equation, within the rectangular barrier, can be written as [63]

$$\Psi_{\text{bar}}(y, t; E) = \varphi_E(y) \exp\left\{-\frac{iEt}{\hbar}\right\} \exp\left\{-\frac{iV_1}{\hbar\omega} \sin \omega t\right\} \quad (58)$$

Here $\varphi_E = e^{\pm k y}$ is a wave function solution of the time-independent problem $H_0 \varphi_E = E \varphi_E$, with the simpler Hamiltonian H_0 .

As it was shown by Büttiker and Landauer [42], the next stage to find the solution for the oscillating rectangular barrier is to match Eq. (58) with the corresponding solutions at the same energy outside the scattering region. For an electron of energy E impinging on the scattering region, there will be reflected and transmitted waves at the three energies E , $E + \hbar\omega$, and $E - \hbar\omega$. So, if the electron is coming from the left, its wave function in the region to the left of the barrier, $y < -L/2$, will be of the form

$$\begin{aligned} \Psi_{\text{inc+ref}} = & (e^{ik(y+L/2)} + r e^{-ik(y+L/2)}) e^{-iEt/\hbar} + r_+ e^{-ik_+(y+L/2)} \\ & \times e^{-i(E+\hbar\omega)t/\hbar} + r_- e^{-ik_-(y+L/2)} \\ & \times e^{-i(E-\hbar\omega)t/\hbar} \end{aligned} \quad (59)$$

where k_{\pm} are the wavevectors corresponding to the side energy bands, defined as $k_{\pm} = (2m/\hbar^2)^{1/2}(E \pm \hbar\omega)^{1/2}$. Equation (59) represents an incident plane wave of unit amplitude and three reflected waves, one of amplitude r at the incident energy and two of amplitudes r_{\pm} at energies $E \pm \hbar\omega$. To the right of the barrier ($y > L/2$), we have for the transmitted wave

$$\begin{aligned} \Psi_{\text{tra}} = & t e^{ik(y-L/2)} e^{-iEt/\hbar} + t_+ e^{ik_+(y-L/2)} e^{-i(E+\hbar\omega)t/\hbar} \\ & + t_- e^{ik_-(y-L/2)} e^{-i(E-\hbar\omega)t/\hbar} \end{aligned} \quad (60)$$

where t is the transmission amplitude at the energy of the incident wave and t_{\pm} are the transmission amplitudes of the sidebands.

In the barrier, for an infinitesimal amplitude of the time-dependent potential, $V_1 \ll \hbar\omega$, we can expand Eq. (58) to

lowest order in V_1 and represent the wave function in the form

$$\begin{aligned} \Psi_{\text{bar}} = & [Be^{\xi y} + Ce^{-\xi y}]e^{-iEt/\hbar} \left[1 + \frac{V_1}{2\hbar\omega} e^{-i\omega t} - \frac{V_1}{2\hbar\omega} e^{i\omega t} \right] \\ & + [B_+ e^{\xi+y} + C_+ e^{-\xi+y}]e^{-i(E+\hbar\omega)t/\hbar} \\ & + [B_- e^{\xi-y} + C_- e^{-\xi-y}]e^{-i(E-\hbar\omega)t/\hbar} \end{aligned} \quad (61)$$

ξ_{\pm} are the inverse decay lengths for the sidebands, defined as $\xi_{\pm} = (2m/\hbar^2)^{1/2}(V_0 - E \mp \hbar\omega)^{1/2}$. The coefficients r , r_{\pm} , B , B_{\pm} , C , C_{\pm} , t , and t_{\pm} are determined by matching the wave functions and their derivatives at $y = -L/2$ and at $y = L/2$ in the usual manner. Note that the matching conditions must hold for all times; therefore, we have to match each time Fourier component separately. r and t play the role of the static reflection and transmission amplitudes, respectively. Using the standard matching relations, it is straightforward to show that for an almost completely reflecting barrier in the opaque limit, $\xi L \gg 1$, the coefficient t of the static barrier is given by the standard expression [63]

$$\begin{aligned} t = & \frac{4k\xi}{k_0^2} e^{-\xi L} \exp \left\{ -i \arctan \left[\frac{\xi^2 - k^2}{2k\xi} \right] \right\} \\ & \times \exp \left\{ i \left[y - kL - \frac{Et}{\hbar} \right] \right\} \end{aligned} \quad (62)$$

For the transmitted waves at the frequencies $(E/\hbar) \pm \omega$, Büttiker and Landauer found that their transmission coefficients are

$$\begin{aligned} t_{\pm} = & \mp t \frac{V_1}{2\hbar\omega} (e^{\pm\omega\tau} - 1) \\ & \times \exp \left\{ i \left[k_{\pm} \mp \frac{m\omega L}{2\hbar} - \frac{(E \pm \hbar\omega)t}{\hbar} \right] \right\} \end{aligned} \quad (63)$$

$\tau = mL/\hbar\xi$ is the time it would take a particle with the velocity $v = \hbar\xi/m$ to traverse the opaque rectangular barrier. To obtain Eq. (63) it was additionally assumed that $\hbar\omega \ll E$, so that the wavevectors of the sidebands are approximately equal to $k_{\pm} \cong k \pm m\omega/\hbar k$, and also that $\hbar\omega \ll V_0 - E$, so that the decay lengths satisfy $\xi_{\pm} = \xi \mp m\omega/\hbar\xi$.

Note that for opaque barriers the traversal time τ^{BL} obtained in the Larmor clock approach, Eq. (14), coincides with the expression considered in the previous equation, $\tau = mL/\hbar\xi$. The classical time that one would obtain in the WKB limit at energies below the peak of the barrier is given by the integral

$$\tau = \int_{y_1}^{y_2} \frac{m}{\hbar\xi(y)} dy = \int_{y_1}^{y_2} \left\{ \frac{m}{2(V_0(y) - E)} \right\}^{1/2} dy \quad (64)$$

where y_1 and y_2 are the classical turning points. This result also reduces to the value appearing in Eq. (63) for the case of a rectangular barrier, when $V_0(y)$ is constant.

The probability of transmission at the sideband energies, determined from Eq. (63), is

$$T_{\pm} = |t_{\pm}|^2 = \left(\frac{V_1}{2\hbar\omega} \right)^2 (e^{\pm\omega\tau} - 1)^2 T \quad (65)$$

where T is the transmission coefficient for the static barrier. For small frequencies, so that $\omega\tau \ll 1$, the probabilities of transmission for the upper and lower sidebands obtained from Eq. (65) are the same and equal to

$$T_{\pm} = \left(\frac{V_1\tau}{2\hbar} \right)^2 T \quad (66)$$

Remember that τ is the approximate expression for the Büttiker–Landauer time for an opaque barrier, given by Eq. (14).

At high frequencies, the upper sideband is exponentially enhanced, while the lower sideband is exponentially suppressed. So for an opaque barrier we do indeed have a rather well-defined crossover between tunnelling at high frequencies and tunnelling at low frequencies, with the characteristic time corresponding to the value given by Eq. (14). This characteristic crossover time is the same one appearing in the expression of the transmission coefficients of the sidebands in the adiabatic limit.

3.2.1. General Barrier

Let us briefly discuss the results of the general oscillating barrier problem following the papers of Hauge and Støvneng [4] and [62]. It was shown that in the adiabatic limit, $\omega \rightarrow 0$, the expression for the transmission coefficients for the sidebands, Eq. (65), can be generalized in the form

$$T_{\pm} = |t_{\pm}|^2 \rightarrow \left(\frac{V_1 |\tau^{\bar{V}}|}{2\hbar} \right)^2 |t(E, \bar{V})|^2 \quad (67)$$

where $|t|^2 = T$ and we have written explicitly the E and \bar{V} dependence of the transmission amplitude t . \bar{V} is the average value of the barrier potential in the scattering region, that is,

$$\bar{V} \equiv \frac{1}{L} \int_{-L/2}^{L/2} V(y) dy. \quad (68)$$

$\tau^{\bar{V}}$ is a complex quantity, with the dimensions of time, defined as

$$\tau^{\bar{V}} = i\hbar \frac{\partial \ln t(E, \bar{V})}{\partial \bar{V}} \quad (69)$$

This quantity characterizes the crossover from the adiabatic to the high-frequency limits, and we define it as the traversal time in the time-modulated barrier approach.

The corresponding definition of the reflection time appeals to the adiabatic limit of the reflected sidebands. Their reflection coefficients $R_{\pm} = |r_{\pm}|^2$ tend in the adiabatic limit to an expression that can be written as

$$|r_{\pm}|^2 \rightarrow \left(\frac{V_1 |\tau_{\text{R}}^{\bar{V}}|}{2\hbar} \right)^2 |r(E, \bar{V})|^2 \quad (70)$$

where $|r|^2 = R$ is the static reflection coefficient. Again, we have explicitly written the E and \bar{V} dependence of the

reflection amplitude r . $\tau_{\text{R}}^{\bar{V}}$ is a new complex quantity, playing the role of a reflection time, defined as

$$\tau_{\text{R}}^{\bar{V}} = i\hbar \frac{\partial \ln r(E, \bar{V})}{\partial \bar{V}} \quad (71)$$

The complex times $\tau^{\bar{V}}$ and $\tau_{\text{R}}^{\bar{V}}$ are related to the real quantities $\tau_{\text{z}}^{\text{BL}}$, $\tau_{\text{y}}^{\text{BL}}$, $\tau_{\text{y,R}}^{\text{BL}}$ and $\tau_{\text{z,R}}^{\text{BL}}$ and therefore the BL traversal time can be formally written in the form

$$\tau^{\text{BL}} \equiv \hbar \left| \frac{\partial \ln t(E, \bar{V})}{\partial \bar{V}} \right| \quad (72)$$

It is still not so clear how this time, which was obtained from an analysis of the time-modulated barrier and which is valid for an arbitrary shaped potential $V(y)$, whose average is \bar{V} , can be justified as a traversal time for a general barrier [64]. In any case, note that Eq. (72) for an opaque barrier leads us to Eq. (14), which was obtained by Büttiker's analysis of the Larmor clock [36]. The BL reflection time can be defined as in Eq. (72), but replacing $t(E, \bar{V})$ by $r(E, \bar{V})$.

3.3. Complex Time

Although common sense dictates that the tunnelling time must be a real time and that there are no clocks that measure a complex time, nevertheless the concept of complex time in the theory of the traversal time problem of electrons appeared in many approaches (see [65], and references therein). The optical analog of the Larmor clock for classical electromagnetic waves based on Faraday effect lead us also to a complex time [37].

We saw, with the help of the GF formalism, that the two characteristic times appearing in the Larmor clock approach correspond to the real and imaginary components of a single quantity, which we define as a complex traversal (or reflection) time. In the subsection on the oscillatory incident amplitude, we also discussed that Leavens and Aers [51] arrived at a complex barrier interaction time, Eq. (52), by studying the shape distortion of the transmitted wave by the barrier.

It is in the Feynman path-integral approach where the concept of a complex time arises more naturally. Sokolovski and Baskin [55], using this kinematic approach to quantum mechanics, showed that a formal generalization of the classical time concept to the traversal time led to a complex quantity. The starting point for the Feynman path-integral approach [57] to the traversal time problem is the classical expression for the time that the particle spends in an arbitrary region $[0, L]$, which can be calculated through the expression

$$\tau_{0L}^{\text{cl}} = \int_0^{\tau} \theta(y(t')) \theta(L - y(t')) dt' \quad (73)$$

where θ is here the step function, equal to 1 when its argument is positive and zero otherwise. The two θ functions ensure that we only count the time while the particle is in the barrier region. To use Eq. (73) in the quantum regime one has to generalize the expression for the classical time by replacing the classical trajectory $y(t)$ in the previous expression by a Feynman path and average Eq. (73) over all possible paths that start at position 0 on the left side of the barrier

and end at position L at time t . Each path is weighted by the quantity $\exp(iS\{y\})$, where

$$S\{y(t)\} = \int_0^t \left(\frac{m}{2} \left(\frac{dy}{dt'} \right)^2 - V(y(t')) \right) dt' \quad (74)$$

is the action associated with the path $y(t)$. As we are weighting each trajectory with a complex factor, it is natural to obtain a complex result for the average value. This weighting assumption has generated some controversies [4, 11, 66, 67]. Sokolovski and Baskin [55] arrived at the following complex time:

$$\tau_{0L} = i\hbar \int_0^L \frac{\delta \ln t}{\delta V(y)} dy \quad (75)$$

where $\delta/\delta V(y)$ represents the functional derivative with respect to the barrier potential.

This result, Eq. (75), is strictly equivalent to our expression of the traversal time. We would like to emphasize that this coincidence is quite natural, because in the tunnelling time problem we always deal with an *open* and *finite* system. The functional derivative with respect to the potential appearing in Eq. (75) is equivalent to a derivative with respect to energy plus a correction term proportional to the reflection coefficient (see Eq. (25)).

The modulus of this expression, Eq. (75), is the time that Büttiker [36] obtained for the tunnelling time in a square potential barrier and related to the Larmor clock times via

$$\text{Re } \tau_{0L} = \tau_{\text{y}} \quad (76)$$

$$-\text{Im } \tau_{0L} = \tau_{\text{z}} \quad (77)$$

Sokolovski and Connor [68] extended the Feynman path-integral approach to include the treatment of wavepackets. In their method the complex tunnelling formally appears as a transition element $\tau_{0L} = \langle \Psi_{\text{F}} | \tau^{\text{cl}} | \Psi_{\text{I}} \rangle$ between the initial wavepacket Ψ_{I} and the final one Ψ_{F} . Nevertheless, we have to note that Feynman and Hibbs [57] themselves do not associate any physical significance to transition elements.

Fertig [69, 70] avoided the problem of having to use wavepackets by considering restricted operators, for a fixed energy or for a fixed time. In this way, he was able to evaluate exactly the amplitude distribution for the traversal time for a rectangular barrier. He assumed that the weight of each path is proportional to $\exp(iS\{y\})$, where the action S is given by Eq. (74). He obtained the following amplitude distribution for the traversal time [70]:

$$F(\tau) = \frac{1}{2\pi t(E, V_0)} \int_{-\infty}^{\infty} e^{-i\omega\tau} t(E, V_0 - \omega) d\omega \quad (78)$$

where $t(E, V_0)$ is the transmission amplitude at energy E through a barrier of height V_0 . With this probability amplitude distribution for the average traversal time for the square potential barrier, he arrives at

$$\langle \tau \rangle = -\frac{d\varphi}{dV_0} + \frac{i}{2} \frac{d \ln T}{dV_0}$$

which is the result of Sokolovski and Baskin [55].

The Wigner path distribution provides another approach to compute the traversal time. Jensen and Buot [71] used it

to calculate the time for stationary waves, and Muga et al. [72] for wavepackets.

Yamada [73] claimed that the probability distribution of the tunnelling time cannot be properly defined. He arrived at this conclusion from the fact that Gell-Mann and Hartle's weak decoherence condition [74] does not hold for the tunnelling time due to the absence of a classical, dominant Feynman path. Yamada defined a range of values of the time and concluded that it is the only "speakable" magnitude.

Sokolovski [75] criticized the previous results on the grounds that the weak decoherence criterion is too restrictive. He showed that the probabilities for the outcomes of tunnelling time measurements can be described in terms of positive-operator-valued measurements, related to the interaction between the system and its environment.

3.3.1. Complex Time and Kramers-Kronig Relations

As it has just been shown, the concept of a complex time in the theory of the traversal time problem of electrons and electromagnetic waves (EMWs) has arisen in many approaches [4, 11, 37, 65]. In [37] was obtained, with the Faraday rotation scheme, a very similar result to Eq. (25) for the characteristic interaction time τ of an EMW. The Faraday rotation in the finite system, which is our magnetic clock, plays for light the same role as the Larmor precession for electrons [34, 36]. The emerging EMW is elliptically polarized and the major axis of the ellipse is rotated with respect to the original direction of polarization. All relevant information about both the angle of rotation and the degree of ellipticity is contained in a complex angle whose real part corresponds to the Faraday rotation, and whose imaginary part corresponds to the degree of ellipticity. This motivated us to associate a complex interaction time of the light in the region with magnetic field which can be written in terms of derivatives with respect to frequency as [37]

$$\tau(\omega) = -i \left[\frac{\partial \ln t}{\partial \omega} - \frac{r + r'}{4\omega} \right] = \tau_1(\omega) - i\tau_2(\omega) \quad (79)$$

As was shown by Ruiz et al. [15], this is a general expression for the interaction time of an EMW with a one-dimensional region with an arbitrary index of refraction distribution, independent of the model considered. It can be rewritten in terms of the GF for photons analogously to Eq. (25), because all the general properties of the GF formalism for electrons which lead us to Eq. (25) are valid for any wave (sound or electromagnetic), whenever its propagation through a medium is described by a differential equation of second order [45].

Thus, most approaches indicate that the characteristic time associated with any wave (classical or quantum-mechanical) is a complex magnitude; which of the two components of this complex time is the most relevant depends on the experiment. It was shown in [15] that the real component $\tau_1(\omega)$ corresponds to the traversal time, and the main effect of the imaginary component $\tau_2(\omega)$ is to change the size of the wavepacket. Balcou and Dutriaux [16] experimentally investigated the tunnelling times associated with frustrated total internal reflection of light. They have shown that the real and imaginary parts of the complex tunnelling time

correspond, respectively, to the spatial and angular shifts of the beam. Note that in most tunnelling experiments, instead of electrons, electromagnetic waves were used to exclude interaction effects (see, e.g., [10–23]).

It is known that the frequency dependence of the real and imaginary parts of certain complex physical quantities are interrelated by the Kramers-Kronig relations, for example, the real (dispersive) part of the complex dielectric function $\epsilon(\omega)$ to its imaginary (dissipative) part, the frequency-dependent real and imaginary parts of an electrical impedance, etc. [76]. The derivation of these relations is based on the fulfillment of four general conditions of the system: causality, linearity, stability, and that the value of the physical quantity considered is assumed to be finite at all frequencies, including $\omega \rightarrow 0$ and $\omega \rightarrow \infty$. If these four conditions are satisfied, the derivation of Kramers-Kronig relations is purely a mathematical operation which does not reflect any other physical properties or conditions of the system. These integral relations are very general and have been used in the theory of classical electrodynamics, particle physics, and solid-state physics as well as in the analysis of electrical circuits and electrochemical systems.

It is straightforward to show that the complex interaction time, $\tau(\omega)$, Eq. (79), is an analytical function of frequency in the upper half of the complex ω -plane (see, e.g., [76]). In other words, the four conditions mentioned above are fulfilled for the complex time (79) and the following relationship between the $\tau(\omega)$ and its complex conjugate $\tau^*(\omega)$ holds on the real axis (see Eq. (79)):

$$\tau(\omega) = \tau^*(-\omega) \quad (80)$$

which means that the complex interaction time $\tau(\omega)$ has the following properties:

$$\tau_1(\omega) = \tau_1(-\omega), \quad \tau_2(\omega) = -\tau_2(-\omega) \quad (81)$$

Therefore, the real part $\tau_1(\omega)$ is an even function of frequency and can have a finite value at zero frequency (for the slab we have $\tau_1^{\text{sl}}(0) = L/vA$). As for the imaginary part $\tau_2(\omega)$, it is an odd function and must vanish in the limit of zero frequency: $\tau_2(0) = 0$. These conditions imply that the real and imaginary components of the time likewise obey Kramers-Kronig integral relations, and so we may write

$$\tau_1(\omega) - \tau_0 = \frac{2}{\pi} \mathbf{P} \int_0^\infty \frac{y\tau_2(y)}{y^2 - \omega^2} dy \quad (82)$$

$$\tau_2(\omega) = -\frac{2\omega}{\pi} \mathbf{P} \int_0^\infty \frac{\tau_1(y) - \tau_0}{y^2 - \omega^2} dy \quad (83)$$

where \mathbf{P} means principal part and $\tau_0 = Ln/c$, that is, the crossing time in the dielectric system, without any boundary. In particular, if we make $\omega = 0$ in Eq. (83), we arrive at the so-called "macroscopic sum rule" for the complex interaction time

$$\tau_1(0) - \tau_0 = \frac{2}{\pi} \int_0^\infty \frac{\tau_2(y)}{y} dy \quad (84)$$

Thus we see from Eq. (84) that in general if no imaginary component $\tau_2(\omega)$ exists at any frequency, then $\tau_1 = \tau_0$ always holds. In the case of the interaction time in the dielectric

slab, the integral relations (82)–(84) can be verified, using the explicit expressions for the components of time (see Eqs. (85) and (86)).

The validity of the Kramers-Kronig relations for the complex interaction time has a rather deep significance because it may be demonstrated that these conditions are a direct result of the causal nature of physical systems by which the response to a stimulus never precedes the stimulus. It can serve also as a starting point to understand the origin of the complex time, and state that the interaction time for any classical or quantum-mechanical wave will always have two components: the real part $\tau_1(\omega)$ and the imaginary part $\tau_2(\omega)$. At this point it is worth mentioning that the experiments with, for example, undersized waveguides [23, 24] or periodic dielectric heterostructures [9, 10], where the so-called “superluminal velocities” have been observed for the barrier tunnelling time, need to be interpreted carefully.

For the dielectric slab, Eq. (79) leads us to the following expressions for the two time components [37]:

$$\tau_1^{\text{sl}}(\omega) = \frac{T\tau_0^{\text{sl}}}{2A} \left\{ (1 + A^2) + (1 - A^2) \frac{\sin 2\Delta}{2\Delta} \right\} \quad (85)$$

and

$$\tau_2^{\text{sl}}(\omega) = \frac{T\tau_0^{\text{sl}}}{2A} \frac{1 - A^2}{2A} \left\{ (1 - A^2) \frac{\sin 2\Delta}{2} + (1 + A^2) \frac{\sin^2 \Delta}{\Delta} \right\} \quad (86)$$

where $\tau_0^{\text{sl}} = L/v$ is the time that light with velocity $v = c/n_0$ would take to cross the slab, when reflection in the boundaries is not important, $\Delta = \omega\tau_0^{\text{sl}}$, $A = n_1/n_0$, n_0 is the refraction index of the slab, and n_1 is the refraction index of the two semi-infinite media outside the slab. T is the transmission amplitude for the slab in the absence of a magnetic field and is given by [63]

$$T = \left\{ 1 + \left(\frac{1 - A^2}{2A} \sin \Delta \right)^2 \right\}^{-1} \quad (87)$$

The complex time components $\tau_1^{\text{sl}}(\omega)$, Eq. (85), and $\tau_2^{\text{sl}}(\omega)$, Eq. (86), are plotted against one another in the complex plane (see Fig. 6). We see that for small frequencies we have a skewed arc. With increasing frequency, the influence of the second terms in Eqs. (85) and (86), due to boundary effects, becomes less important and the curve, in the limit $\omega \rightarrow \infty$, approximates to an ideal circle.

Note that in the case of the Debye dispersion relations for the complex dielectric function $\epsilon(\omega)$, an ideal semicircle in the complex plane means that we deal with a single relaxation time. In our case it means that for high frequency or short wavelength, we deal with the classical crossing time, taking into account multiple reflection in the slab [15].

It is not difficult to show that in the limit $\omega \rightarrow \infty$ we have

$$(\tau_2^{\text{sl}})^2 + \left\{ \tau_1^{\text{sl}} - \left[\frac{\tau_0^{\text{sl}}}{2A} (1 + A^2) - r \right] \right\}^2 = r^2 \quad (88)$$

which is the equation of a circle in the complex plane of $-\tau_2^{\text{sl}}$ and τ_1^{sl} with the center $\{\tau_0^{\text{sl}}/2A(1 + A^2) - r, 0\}$ and with a radius given by

$$r = \frac{\tau_0^{\text{sl}} (1 - A^2)^2}{4A (1 + A^2)}$$

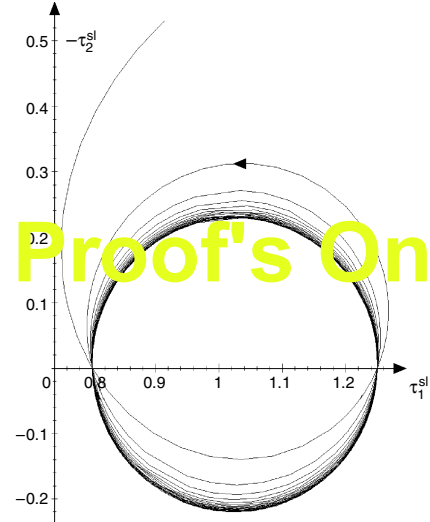


Figure 6. Complex plane interaction time diagram for a dielectric slab. The arrow indicates the direction of increasing frequency. Reprinted with permission from [86], V. Gasparian et al., “Handbook of Nanostructured Materials and Nanotechnology” (H. S. Nalwa, Ed.), Vol. 2, Chapter 11, 1999. © 1999, Elsevier Science.

Thus the two components, the real part $\tau_1(\omega)$ and the imaginary part $\tau_2(\omega)$, of the complex barrier interaction time for EMW are not entirely independent quantities, but connected by Kramers-Kronig relations. This means that the response to a stimulus never precedes the stimulus and thus the experiments [9, 10, 23, 24], where the so-called “superluminal velocities” have been observed need to be interpreted with respect to the fact that any classical or quantum-mechanical wave will always have two components; which of the two components is the most relevant depends on the experiment.

The validity of the Kramers-Kronig relations was only checked analytically for EMW, but in general this implies that they are also valid for all quantum particles represented by a differential equation of second order as indicated by the numerical calculations for the complex tunnelling time for electrons.

3.4. Escape Time of Electrons from Localized States

As we have seen in most approaches of the tunnelling time problem, only the scattering configuration in which the free electron (or wavepacket) is coming from the left (right) on a 1D arbitrary potential barrier has been considered. More than one tunnelling time is involved in this time problem, no matter whether we deal with the Büttiker-Landauer τ^{BL} or complex $\tau = \tau_1 - i\tau_2$ characteristic times (see Eqs. (12) and (24)). Furthermore, this seems not to be a peculiarity of a quantum-mechanical wave, but a general result, as the characteristic time associated with a classical wave is also a complex magnitude [37]. Which of the two components of this complex time is the most relevant depends on the experiment. For photons [37], the real part is proportional to the Faraday rotation or the density of optical modes, while the

imaginary part gives the degree of ellipticity. In [16] the tunnelling times associated with frustrated total internal reflection of light were experimentally investigated, and the real and imaginary parts of the complex tunnelling time were shown to correspond to the spatial and angular shifts of the beam, respectively.

On the other hand, it is clear that there are other similar situations of practical interest which should be discussed in the same context of two time components as was done in the scattering problem. One of these situations is the escape of an electron from localized states in a quantum well with one or several surrounding barriers. The escape of an electron from a localized state in the quantum well connected to a continuum by a small barrier only by one side (Fig. 7) can be found, for instance, in miniaturized metal-oxide-semiconductor transistors, in which electrons arrive to the quantized accumulation or inversion layers after scattering and subsequently they can tunnel to the metal gate through a very narrow oxide layer which acts as the barrier [77]. Physically, this implies that the particles entering the quantum well region remain there for some time before being allowed to escape outside. Tunnelling escaping time has also been studied by transient-capacitance spectroscopy [78], where electrically injected electrons undergo an escaping process out of the quantum well, for example, in a three-barrier, two-well heterostructure [79, 80].

Let us consider a potential shape that includes a well and one surrounding barrier (see Fig. 7). A hard wall condition at $x = -w$ reduces the problem to escape to only one open channel, that is, transmission to the right.

To calculate the escape time $\tau^{\text{esc}}(k)$ of an electron from a quantum well when boundary effects can be neglected, we closely followed [81] and introduced the following complex quantity ($k = \sqrt{E}$):

$$\tau^{\text{esc}}(k) = -i \frac{d \ln t}{2k dk} \quad (89)$$

where $t = T^{1/2} e^{i\phi}$ is the complex amplitude of transmission of the electron through only the right barrier taking into account the hard wall condition at $x = -w$.

Using standard methods of quantum mechanics, it is easy to show that the Re and Im parts of the complex escape time

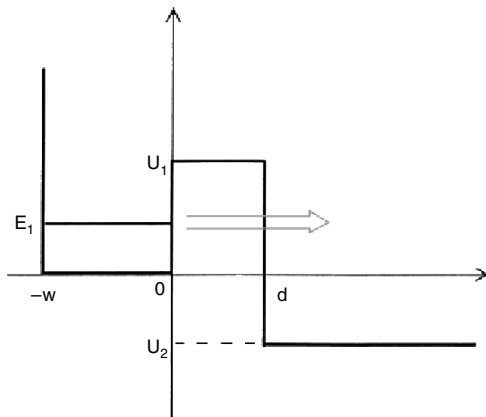


Figure 7. Schematic representation of the simplified potential profile, with a hard wall condition at $-w$.

$\tau^{\text{esc}}(k) = \tau_1^{\text{esc}}(k) - i\tau_2^{\text{esc}}(k)$ of an electron from a quantum well when boundary effects can be neglected and near the resonance energy E_1 and in the limit of an opaque barrier ($\gamma d \gg 1$) are given by [81]

$$\tau_1^{\text{esc}}(k_1) = \frac{\xi(1+\gamma w)(1+\beta^2)}{2k^2(1+\xi^2)} \exp(2\gamma d) \quad (90)$$

$$\tau_2^{\text{esc}}(k_1) = \frac{(1+\gamma w)(1+\beta^2)(1-\xi^2)}{4k^2(1+\xi^2)} \exp(2\gamma d) \quad (91)$$

where $\xi = \gamma/k_3$, $\gamma = \sqrt{E_1 - U_2}$, $\beta = k_1/\gamma$, and w, d, U_1, U_2 are defined in Figure 7.

Let us examine the relationship between the two components we have defined above and the lifetime expression

$$\tau_{\text{LT}}(k_1) = \frac{(1+\gamma w)(1+\beta^2)(1+\xi^2)}{16 \cdot k_1^2 \cdot \xi} \exp(2\gamma d) \quad (92)$$

which follows from an approximate perturbative approach based on Bardeen's perturbation Hamiltonian [82].

Despite the similarity between Eqs. (90), (91), and (92), they only allow a qualitative comparison at the bound level E_1 . Since components τ_1^{esc} and τ_2^{esc} show a sharp variation around this energy, a comparison with Eq. (92) as a function of energy is interesting in order to study their behavior at the quasi-bound level, which is shifted with respect to E_1 . Such comparison is shown in Figure 8 for the following parameter values: $U_1 = 1$, $U_2 = -1$, $w = 3$, for two d values ($d = 5$ in Fig. 8a, and $d = 2$ in Fig. 8b). An opaque barrier has been

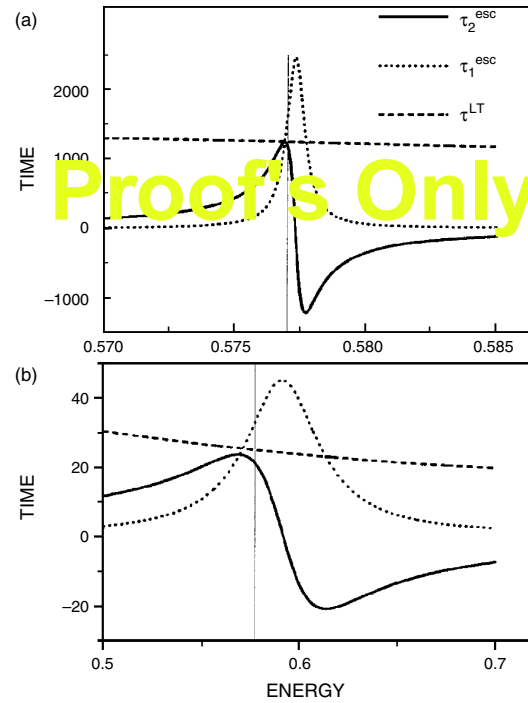


Figure 8. The time components as a function of energy for the potential profile depicted in Figure 7, with $U_1 = 1$, $U_2 = -1$, and $w = 3$, for two different d values: (a) $d = 5$, and (b) $d = 2$. The vertical line corresponds to the ground energy level when the barrier width is infinite. Reprinted with permission from [81], J. A. Lopez Villanueva and V. Gasparian, *Phys. Lett. A* 260, 286 (1999). © 1999, Elsevier Science.

chosen in Figure 8a to ensure the accuracy of the lifetime expression, but in Fig. 8b the estimated relative error for the lifetime expression is about 16%. The vertical line corresponds to the ground energy level when the barrier width is infinite. It is seen that the maximum of component τ_2^{esc} coincides with the τ_{LT} lifetime expression (92) at an energy very close to the bound level in the opaque barrier case (Fig. 8a). With the narrow barrier (Fig. 8b) both results deviate, but in this case the lifetime expression overestimates the lifetime by about 16% while the maximum of component τ_2^{esc} still provides an accurate value. Furthermore, this maximum is produced at an energy lower than the bound level, as predicted by the first-order perturbation theory.

Let us represent the complex time components $\tau_1^{\text{esc}}(k)$ and $\tau_2^{\text{esc}}(k)$ in the complex E plane. They are plotted against one another in Figure 9 and as it is seen, provide ellipse. This is what we expected, as the maxima of $\tau_1^{\text{esc}}(k)$ and $\tau_2^{\text{esc}}(k)$ are not the same. Nevertheless, there is a property of an ellipse that could be interesting: it is symmetric with respect to its main axis. Therefore, the maximum (and the minimum) of $\tau_2^{\text{esc}}(k)$ are found at the points where $\tau_1^{\text{esc}}(k)$ has a value of half its maximum. As this value is used to compute lifetime (width of the $\tau_1^{\text{esc}}(k)$ peak at half height), this width must be exactly the difference in energies between the maximum and minimum of $\tau_2^{\text{esc}}(k)$. It is easy to check that we have the following condition:

$$(E_{\min} - E_{\max})\tau_2^{\text{esc}} = 1$$

which confirms our previous conclusion concerning the fact that τ_2^{esc} at an energy close to the bound level in the well, coincides with the lifetime expression.

3.5. Wavepacket Approach

The delay time of a particle through a region can be directly calculated by following the behavior of its wavepacket. This approach has been criticized from different points of view, mainly due to the lack of causal relationship between the peaks or the centroids of the incident and transmitted wavepackets, and also because of the difficulties of an experimental setup to measure delay times. The dispersive character of electron propagation has been claimed as responsible for the acceleration of wavepackets under appropriate circumstances. High-energy components of the

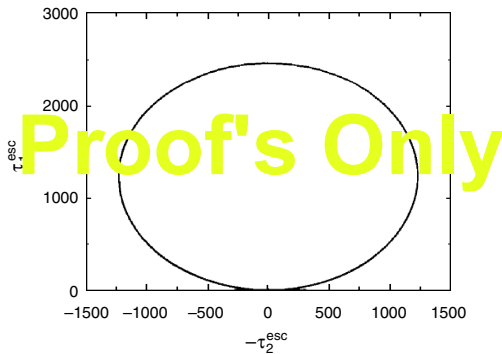


Figure 9. Complex plane escape time diagram for the quantum well used in this chapter.

packet travel faster and are transmitted more effectively than the other components, and so the transmitted packet comes almost entirely from the front of the incident packet. However, similar results were also obtained for dispersive electromagnetic waves [15]. The fact that the transmitted wavepacket comes from the beginning of the incident wavepacket is mainly a consequence of interference effects. The results obtained from the wavepacket approach are similar to the results obtained with other approaches, and can be easily generalized to include finite size effects. In this section we review how to obtain delay times from the transmission coefficients.

Let us assume a region of interest, which in principle can be of any dimensionality, coupled to the outside by two 1D leads with a constant potential that we will assume equal to zero. We choose a coordinate system such that the incident lead extends from $-\infty$ to 0, and the other lead from L to $+\infty$. A gaussian wavepacket of spatial width σ_1 is incident from the incoming lead on the region of interest. This packet is characterized by a wave function of the form

$$\Psi(y, t) = \int_{-\infty}^{\infty} C \exp[-(k - k_0)^2/2(\Delta k)^2] \times \exp[iky - i\omega t] dk \quad (93)$$

where C is a normalization constant, k_0 is the central wavenumber, $\omega = E/\hbar$, and $\Delta k = 1/\sqrt{2}\sigma_1$ is the spread of the packet in the wavenumber domain. The time evolution of this wavepacket is governed by the Schrödinger equation, although the results are directly applicable to any other type of wave, including classical electromagnetic waves. Part of the packet is transmitted and continues travelling outward along the second lead. Its wave function is given by

$$\Psi_t(y, t) = \int_{-\infty}^{\infty} C |t(k)| e^{i\varphi(k)} \exp[-(k - k_0)^2/2(\Delta k)^2] \times \exp[iky - i\omega t] dk \quad (94)$$

$t(k)$ is the amplitude of transmission and $\varphi(k)$ is its phase, which here we prefer to write as functions of the wavenumber k . The functions $t(k)$ and $\varphi(k)$ contain all the relevant information to calculate the delay time of the electronic wave function due to the region of interest.

The general solution for finite size wavepackets has to be obtained numerically, but we can get close expressions for the delay time in the limit of very long wavepackets from a series expansion along the central wavenumber k_0 . Let us assume that the wavepacket is so long (and so Δk so small) that $t(k)$, $\varphi(k)$, and $\omega(k)$ only change smoothly on the scale of Δk . Then, in evaluating $|\Psi_t(y, t)|^2$, where $\Psi_t(y, t)$ is given by Eq. (94), we can expand $t(k)$, $\varphi(k)$, and $\omega(k)$ to second order in $k - k_0$. We write the phase of the transmission amplitude as

$$\varphi(k) = \varphi(k_0) + \tau_1(\omega - \omega_0) + \frac{1}{2}\tilde{\tau}_1(\omega - \omega_0)^2 \quad (95)$$

where ω_0 is the frequency corresponding to the central wavenumber, τ_1 is the first derivative of the phase $\tau_1 = d\varphi(\omega)/d\omega$, which roughly corresponds to the component τ_y of the Büttiker-Landauer time, and $\tilde{\tau}_1$ is its second

derivative $\tilde{\tau} = d^2\varphi(\omega)/d\omega^2$. Analogously, we write the modulus of the transmission amplitude as

$$|\log t(k)| = |\log t(k_0)| + \tau_2(\omega - \omega_0) + \frac{1}{2}\tilde{\tau}_2(\omega - \omega_0)^2 \quad (96)$$

where $\tau_2 = d|\log t(\omega)|/d\omega$, and $\tilde{\tau}_2 = d^2|\log t(\omega)|/d\omega^2$. We can also expand the frequency ω in terms of k :

$$\omega = \omega_0 + v_g(k - k_0) + \frac{1}{2}a_g(k - k_0)^2 \quad (97)$$

v_g is the group velocity $v_g = d\omega/dk$, and a_g is its derivative with respect to k , $a_g = d^2\omega/dk^2$. For electrons, the group velocity is equal to $v_g = \hbar k/m$, while the group acceleration is $a_g = \hbar/m$.

If we keep terms up to second order in $k - k_0$, we can do analytically all the integrals appearing in the expression of the average value and the variance of y . After some trivial calculations we obtain that the average position $\langle y \rangle$ of the transmitted wavepacket as a function of time is given by

$$\langle y \rangle = (t - \tau_1)v_g \left[1 + \frac{\tau_2 a_g}{b} \right] - \frac{\tau_2 \tilde{\tau}_1 v_g^3}{b} \quad (98)$$

where b is equal to

$$b = \frac{1}{(\Delta k)^2} - \tau_2 a_g - \tilde{\tau}_2 v_g^2 \quad (99)$$

We have chosen the phase of the incident wavepacket so that its peak is at the origin of coordinates in $t = 0$, in the absence of perturbations due to the presence of the barrier, that is, $\langle y_i \rangle(t = 0) = 0$. The peak of the transmitted wavepacket would be at the same position at a time τ implicitly defined by

$$\tau = t(\langle y_t \rangle = 0) \quad (100)$$

The barrier delays the gaussian wavepacket by an amount of time τ , which according to Eqs. (100) and (98) is equal to

$$\tau = \tau_1 + \tau_2 \tilde{\tau}_1 v_g^2 (\Delta k)^2 \quad (101)$$

This equation constitutes a useful tool for calculating the tunnelling time of an electron that has transversed a (rectangular) barrier as a function of the width of the incident wavepacket, Δk .

We can express Eq. (101) in terms of Büttiker–Landauer's times and their first derivatives. If we neglect the terms proportional to the reflection amplitudes in the expressions for Büttiker–Landauer's times, we have $\tau_1 = \tau_y$ and $\tau_2 = \tau_z$. Taking into account the dispersion relation for electrons, we also have

$$\tilde{\tau}_1 = \frac{1}{v_g} \tilde{\tau}_y \quad (102)$$

and a similar expression for τ_2 and τ_z . Thus Eq. (101) can be rewritten in the form

$$\tau = \tau_y + \tau_z \tilde{\tau}_y v_g (\Delta k)^2 \quad (103)$$

This is the main result of the long wavepacket approximation up to second order in Δk . We will check the limit of validity of this expression in the section on numerical results.

3.6. Time-of-Arrival Operator Approach

A direct attempt to obtain an observable for the time runs into the problem pointed out by Pauli [83] that the existence of such an operator would imply an unbounded energy spectrum, given the uncertainty relation between time and energy. The time-of-arrival is the natural candidate to become a property of the system, rather than an external parameter, and it plays a role similar to our traversal time.

Leon et al. [84, 85] have recently developed an interesting time-of arrival formalism, which we briefly describe. Classically, the time-of-arrival of a particle with coordinate q and momentum p at a point x is given by the expression

$$t_x(q, p) = \text{sgn}(p) \sqrt{\frac{m}{2}} \int_q^x \frac{dq'}{\sqrt{H(q', p) - V(q')}} \quad (104)$$

where $H(q, p)$ is the classical hamiltonian. Leon et al. (1996) showed that $t_x(q, p)$ is canonically conjugate to the hamiltonian $\{t_x(q, p), H(q, p)\} = -1$, where $\{\}$ are the Poisson brackets, but were unable to quantize this magnitude directly. Instead they considered first the time-of arrival for a free particle $t_{x0}(q, p) = m(x - q)/p$, which after symmetrization is quantized as

$$t_{x0}(q, p) = -e^{-ipx} \sqrt{\frac{m}{p}} q \sqrt{\frac{m}{p}} e^{ipx} \quad (105)$$

This operator is not self-adjoint, a difficulty related to the Pauli theorem. The measurement problem associated to the time-of-flight operator can be solved by means of a positive-operator-valued measure.

As a second step, Leon et al. [84] considered the canonical transformation that connects the free particle system with the general system including a potential $V(q)$. The Möller operators perform this canonical transformation. They are normally used to connect the free particle wavefunctions with the scattering and bound states of a given potential. In their formalism, Leon et al. applied these unitary operators to the time-of-arrival operator of the free particle in order to produce the corresponding operator in the presence of an arbitrary potential. Given this operator, one can then obtain the full distribution for the time-of-arrival of a particle at a position.

We believe that an especially interesting result of their approach is the average value of the time-of-arrival for a particle originally in state $\psi(k)$ which traverses a barrier with amplitude $\hat{t}(k)$. The expected average value is equal to

$$\tau = \frac{\int_{-\infty}^{\infty} dk |\hat{t}(k) \tilde{\psi}(k)|^2 \tau_y(k)}{\int_{-\infty}^{\infty} dk |\hat{t}(k) \tilde{\psi}(k)|^2} \quad (106)$$

where $\tilde{\psi}(k)$ is the Fourier transform of $\psi(k)$. This expression has a very intuitive interpretation. The time corresponds to an average of the characteristic time τ_y over the transmitted components of the wavepacket. It is very easy to calculate this expression and can be applied to packets of any size. In the section on numerical results we will estimate the validity of this expression.

4. NUMERICAL RESULTS

The long wavepacket limit, when the spread of the wave function is longer than the size of the system, is well understood [86]. In all cases studied, the traversal and the reflection times correspond to the real component of time, τ_y . In this limit, the numerical problem reduces to the evaluation of the transmission and reflection amplitudes and their energy derivatives, which can be conveniently achieved through the use of the characteristic determinant method, introduced by Aronov et al. [45] and explained in Appendix A. Different similar mathematical methods, allowing us to take into account multiple interfaces consistently and exactly without the use of perturbation theory, have been proposed [87–91].

Numerical simulations are needed to clarify finite size effects. In this case we have to consider a specific wavepacket and evaluate its probability amplitude at different values of the time in order to calculate the amount of time taken to cross the system. In this section, we first review the results for periodic structures which, due to their complexity, are treated as nondispersive media, and so the conclusions are directly applicable to electromagnetic waves. Second, we consider the case of resonant tunnelling and we finish by presenting the results for finite size effects in electron tunnelling.

4.1. Periodic Structure

Let us consider a periodic arrangement of layers with potential V_1 and thickness d_1 alternating with layers with potential V_2 and thickness d_2 . We assume that the energy is higher than $\max\{V_1, V_2\}$, and so the wavenumber in the layers of the first and second type is $k_i = [2m(E - V_i)]^{1/2}/\hbar$ ($i = 1, 2$). In this case, the results for long wavepackets apply equally well to electromagnetic waves considering $k_i = \omega n_i/c$, where n_i is the index of refraction of the two types of layers. We concentrate on the simplest periodic case, which corresponds to the choice $k_1 d_1 = k_2 d_2$. This case contains most of the physics of the problem and is also used in most experimental setups [9]. Let us call a the spatial period, so $a = d_1 + d_2$. The periodicity of the system allows us to obtain analytically the transmission amplitude using the characteristic determinant method [40]:

$$t = e^{-ik_1 d_1} \left\{ \cos(N\beta a/2) - i \frac{\sin(N\beta a/2)}{\sin \beta a} \times \sqrt{\sin^2 \beta a + \left[\frac{k_1^2 - k_2^2}{2k_1 k_2} \sin k_2 d_2 \right]^2} \right\}^{-1} \quad (107)$$

where β plays the role of quasi-momentum of the system, and is defined by

$$\cos \beta a = \cos k_1 d_1 \cos k_2 d_2 - \frac{k_1^2 + k_2^2}{2k_1 k_2} \sin k_1 d_1 \sin k_2 d_2 \quad (108)$$

When the modulus of the RHS of Eq. (108) is greater than 1, β has to be taken as imaginary. This situation corresponds to a forbidden energy band. The term within brackets in Eq. (107) only depends on the properties of one barrier, while the quotient of the sine functions contains the information about the interference between different barriers. The transmission coefficient is equal to 1 when $\sin(N\beta a/2) = 0$ and β is different from 0. This condition occurs for

$$\beta a = \frac{2\pi n}{N} \quad (n = 1, \dots, N/2 - 1) \quad (109)$$

and we say that it corresponds to a resonant frequency.

For the reflection amplitude we have

$$r = t e^{-ik_1 d_1} \frac{k_1^2 - k_2^2}{2k_1 k_2} \sin k_2 d_2 \frac{\sin(N\beta a/2)}{\sin \beta a} \quad (110)$$

With these expressions for the transmission amplitude, Eq. (107), and for the reflection amplitude, Eq. (110), we can calculate the traversal time through Eq. (25) and the reflection time via Eq. (31). From Eqs. (107) and (110), Ruiz et al. [15] calculated numerically the traversal time for electromagnetic waves considering a system of 19 layers ($N = 20$) with alternating indices of refraction of 2 and 1, and widths of 0.6 and 1.2, respectively. Their main conclusions are also applicable to the problem of an electron in a periodic potential. In Figure 10 we represent τ_1 and τ_2 for electromagnetic waves in a periodic system as a function of k_1 . In the energy gaps, the traversal times are significantly smaller than the crossing time at the vacuum speed of light (horizontal line). The average of τ_1 with respect to wavenumber is equal to 22.8, and coincides with the classical crossing time, that is, for very short wavepackets, without including multiple reflections. It corresponds to the horizontal straight line in Figure 10.

The kinetic approach is suitable to study numerically the evolution of wavepackets with sizes of the order of the width of the region of interest. We will describe the numerical simulations of the time evolution of finite size wavepackets that cross the region of interest and measure the delay of the peak of the transmitted wave as a function of the size of the

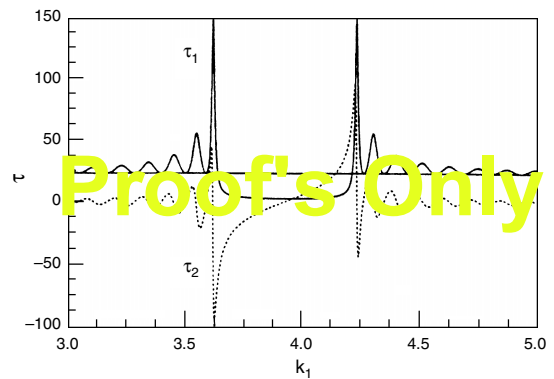


Figure 10. Traversal times versus the size of the wavepacket for a periodic system. The solid line corresponds to τ_1 , and the dashed line to τ_2 . The values of the parameters are $N = 20$, $n_1 = 2$, $n_2 = 1$, $d_1 = 0.6$, and $d_2 = 1.2$.

original packet. The simulations also calculate the change in size of the packets. First we consider the results for periodic structures without including dispersion effects, so we will use a nomenclature most appropriate for electromagnetic waves, although the results are equally valid for electrons, in the absence of dispersion, provided that we translate indices of refraction into their corresponding potentials. Later we will also present results about finite size effects in electron tunnelling.

Let us consider a three-dimensional layered system with translational symmetry in the Y - Z plane, consisting of N layers labelled $i = 1, \dots, N$ between two equal semi-infinite media with a uniform dielectric constant n_0 . The boundaries of the i th layer are given by y_i and y_{i+1} , with $y_1 = 0$ and $y_{N+1} = L$, so that the region of interest corresponds to the interval $0 \leq y \leq L$. Each layer is characterized by an index of refraction n_i . In the case of electrons, we assume that the energy E of the electron is higher than the potentials of the different layers and that the wavenumbers are inversely proportional to the indices of refraction; so the potential V_i in layer y is equal to $V_i = E(1 - (n_0/n_i)^2)$.

One calculates the position of the packet at different times and from this information one extracts the time taken by the packet to cross the region of interest. In particular, neglecting dispersion, one can measure the average positions \bar{y}_1 and \bar{y}_2 of the square of the modulus of the wavepacket at two values of t , t_1 and t_2 , such that the packet is very far to the right of the structure at t_1 and very far to the left at t_2 . These average positions are defined as

$$\bar{y}(t) = \int_{-\infty}^{\infty} y |\Psi(y, t)|^2 dy \quad (111)$$

The traversal time of the wavepacket through the region of interest is given by

$$\tau = t_2 - t_1 - \frac{(\bar{y}_2 - \bar{y}_1 - L)n_0}{c} \quad (112)$$

Although we refer to this time as a traversal time, it is learned that, strictly speaking, it is a delay time. Part of the interest of this type of simulations is to study how delay times relate to the previously obtained expressions for the traversal time.

Figure 11 represents the delay time versus the size of the wavepacket for two values of the central wavenumber, $k_0 = 3.927$ and $k_0 = 4.306$, which correspond to the center of the gap and to a resonance, respectively. There is again a strong similarity in the behavior of the traversal time and of the transmission coefficient [15]. The long wavepacket limit of the traversal time coincides with the characteristic time τ_1 , while the short wavepacket limit is independent of wavenumber and equal to 29. The speed of the wave is greater than in vacuum for a wide range of sizes. The minimum size of the packets that travel faster than in vacuum is about 9, so that the corresponding width $2\sigma_1$ is very much the same as the size of the system. Velocities larger than in vacuum occur when the transmission coefficient is very small. In regions with a very small density of states, the traversal time is very short and, at the same time, transmission is very difficult due to the lack of states at the corresponding energies.

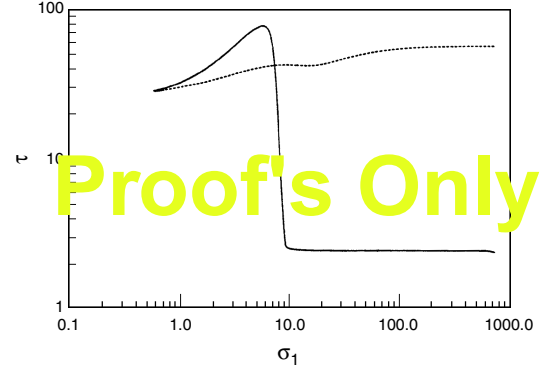


Figure 11. Traversal time versus the size of the wavepacket for a periodic system. The solid line corresponds to a central wavenumber $k = 3.927$, and the dashed line to $k = 4.3$.

The width of the transmitted packet σ_T is slightly smaller than the width of the incident packet σ_1 . According to the results in the subsection on the wavepacket approach, we obtain that, in the absence of dispersion and up to second order in perturbation theory, this change in width depends on the derivatives with respect to frequency of τ_1 and τ_2 . As the first of these derivatives is equal to zero in the center of the gap, one arrives at

$$\sigma_T^2 = \sigma_1^2 - \frac{v_g^2}{2} \frac{d\tau_2}{d\omega} \quad (113)$$

In order to check up to which sizes second-order perturbation theory is valid, Ruiz et al. [15] plotted $\sigma_T^2 - \sigma_1^2$ as a function of the size of the packet and compared it with the value of $(1/2)(d\tau_2/d\omega)$ obtained from the characteristic determinant. Second-order perturbation theory works adequately for a wide range of sizes and, in particular, for the sizes for which one obtains velocities larger than in vacuum. The error in the measurement of the traversal time of a single wavepacket is its width divided by its velocity. All the packets that travel faster than in vacuum are so wide that their uncertainty in the traversal time is larger than the traversal time itself and even larger than the time it would take a wave to cross the structure travelling at the same speed as in the vacuum.

4.2. Resonant Tunnelling

A double-barrier structure is a special case of a periodic system consisting of $N = 4$ interfaces with two evanescent regions separated by a propagating one. In the evanescent layers, the potential energy V_2 is larger than the energy of the electron E . The results of the previous part also applied to this case where one type of layers are evanescent. We merely have to replace k_2 by $-i\kappa$ where $\kappa = [2m(V_2 - E)]^{1/2}/\hbar$. (Correspondingly, $\sin k_2 d_2$ becomes $\sinh \kappa d_2$.) Double-barrier potential structures present resonant tunnelling, which has been studied for electrons since the early days of quantum mechanics [56]. Resonant tunnelling for electromagnetic waves is easier to carry out than corresponding experiments on electrons [24].

The traversal time τ for electromagnetic waves through a double-barrier structure was calculated by Cuevas et al. [40]

using the previous equations for the transmission and reflection amplitudes, Eqs. (107) and (110) with $N = 4$. They considered the finite resolution of the experimental devices by convoluting these expressions with a gaussian distribution function with a standard deviation of 6 MHz, which reproduces the same average height of the peak of the transmission coefficient as the corresponding experiments [24]. They found that at each resonance the Büttiker-Landauer traversal time is basically double the lifetime.

The dependence of the traversal time with frequency at a resonance is fairly universal. The phase of the transmission amplitude changes by an angle of π at each resonance, as predicted by Friedel's sum rule. Its frequency dependence can be fitted quite accurately by an arc tangent function. The time, proportional to the derivative of this phase, is a Lorentzian with the same central frequency and width as the Lorentzian corresponding to the transmission coefficient. As the lifetime τ_1 of the resonant state is the inverse of the width of the transmission coefficient at half maximum, we conclude that it must be equal to half the traversal time at the maximum of the resonant peak:

$$\tau_1 = \frac{1}{2} \tau_{\text{res}} \quad (114)$$

This result was obtained by Gasparian and Pollak [43] by considering the traversal time for an electron tunnelling through a barrier with losses, that is, with a decay time.

4.3. Finite Size Effects in Tunnelling

We have simulated the evolution of a finite wavepacket tunnelling across a rectangular barrier of height V_0 and length L and we have measured the delay of the peak of the transmitted wave as a function of the size of the original packet. The results are used to establish the limit of validity of the long wavepacket approach up to second order and of the time-of-arrival operator approach, previously analyzed.

As we have explained at the beginning of this section, one calculates the position of the packet at different times and from this information one extracts the time taken by the packet to cross the region of interest. Part of the interest of this type of simulations is to study how this time relates to the previously obtained expressions for the traversal time. In Figure 12 we represent the tunnelling time, τ , versus the width of the wavepacket in k -space, Δk , for an incident electron with a momentum $p_0 = 2.6$. The units are set by the choice $\hbar = m_e = 1$. The barrier parameters are $V_0 = 6$ and $L = 15$ (squares), 30 (circles). The numerical results are represented by geometrical figures, each one corresponding to a different barrier length L . The continuous curves represent the results obtained in the large wavepacket approach up to second order, Eq. (103). In the limit $\Delta k \rightarrow 0$ the tunnelling time tends to τ_y and is independent of L , in agreement with the so-called Hartman effect [19]. The continuous curves fit the numerical results relatively well up to values of Δk of the order of $3/L$. This limit of validity is quite general and has been checked for many different values of p_0 , V_0 , and L .

The width of the transmitted packet σ_T is slightly smaller than the width of the incident packet σ_I . According to the results in the subsection on the wavepacket approach,

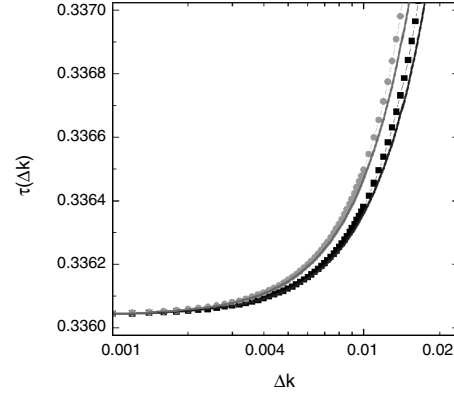


Figure 12. Tunnelling time τ versus the size of the wavepacket Δk for an incident electron with momentum $p = 2.6$ and barrier parameters $V_0 = 6$ and $L = 15$ (squares), 30 (circles). The curves represent the results for the long wavepacket approach up to second order.

we obtain that, up to second order in perturbation theory, this change in width depends on the derivatives with respect to frequency of τ_2 . Second-order perturbation theory works adequately for a wide range of sizes.

We now want to analyze the applicability of the time-of-arrival operator approach previously studied. The average traversal time in this method is given by Eq. (106). Up to second order of approximation, this method coincides with the long wavepacket approach except for a term which depends on the second derivative of the Büttiker time τ_y with respect to the wavenumber k :

$$\tilde{\tau}_y \equiv \frac{\partial^2 \tau_y}{\partial k^2} \quad (115)$$

This term is negligibly small in most practical situations. Then it is feasible that the time calculated via Eq. (106) (to all orders in Δk) constitutes a very good approximation to the exact results.

In Figure 13 we show the tunnelling time τ versus Δk for an incident electron with momentum $p_0 = 2.5$ and rectangular barrier parameters $V_0 = 5$ and $L = 85$. The numerical results are represented by circles and the continuous

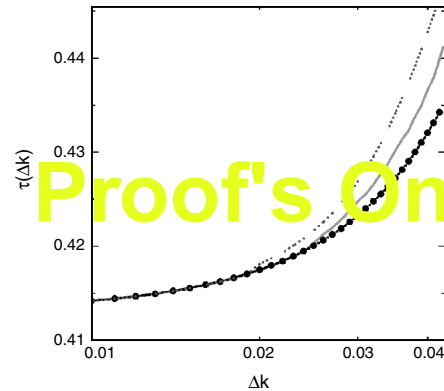


Figure 13. Tunnelling time τ versus Δk for an incident electron with momentum $p = 2.5$ and barrier parameters $V_0 = 5$ and $L = 85$. The numerical simulations (circles) and the results of the time-of-arrival approach (continuous curve) are similar up to sizes $\Delta k = 3.5/L$.

curve corresponds to Eq. (106), while the dashed curve corresponds to the wavepacket approach up to second order. We note that the weighting method fits the numerical results for a larger range of sizes. We estimate that it can be considered an excellent approximation for values of Δk smaller than $3.5/L$. The weighting method is also very practical since it only requires the evaluation of an integral in k and it can be applied to all kind of wavepackets.

5. CONCLUSIONS AND OUTLOOK

In this review we have discussed the topic of tunnelling time in mesoscopic systems including nanostructures, particularly in 1D systems with arbitrary shaped potential. But the treatment of tunnelling time in “nanostructured materials” approaching the molecular and atomic scales is still open. In the field of tunnelling time, there are problems in any of the existing approaches, and we do not have a clear answer for the general question “How much time does tunnelling take?”. Unfortunately no one of these approaches is completely adequate for the definition of the time in QM. Nevertheless, we note that all these different approaches can be consistently formulated in terms of Green’s function, and their main differences can be fairly well understood.

For 1D systems we obtained closed expressions for the traversal and reflection times, Eqs. (25) and (31), in terms of partial derivatives of the transmission and reflection amplitudes with respect to energy. Results of other approaches can be related to these expressions and the main differences can be grouped into two categories: the complex nature of time and finite size effects.

Our conclusion about the complex nature of time is the following. It is clear that there are two characteristic times to describe the tunnelling of particles through an arbitrarily shaped barrier. (Similar conclusions can be reached for reflecting particles.) These two times correspond to the real and imaginary components of an entity, which we can choose as the central object of the theory. They are not entirely independent quantities, but are connected by Kramers-Kronig relations. Different experiments or simulations will correspond to one of their components or to a mixture of both. Büttiker and Landauer argue that these two times always enter into any physically meaningful experiment through the square root of the sum of their squares, and so claim that the relevant quantity is the modulus of the complex time.

As regards finite size effects, we believe that Eqs. (25) and (31) are exact, and adequately incorporate finite size effects. These effects correspond to the terms which are not proportional to derivatives with respect to energy. They are important at low energies and whenever reflection is important (as compared to changes in the transmission amplitude). Several approaches do not include finite size terms, since they implicitly consider very large wave functions. The WKB approximation, the oscillatory incident amplitude approach, and the wavepacket analysis, for example, do not properly obtain finite size effects. On the other hand, our GF treatment, based on the Larmor clock, the generalization of the time-modulated barrier approach, and the

Feynman path-integral treatments arrived at exact expressions. In order to see that these expressions are all equivalent, one has to transform the derivative with respect to the average barrier potential, appearing in the time-modulated barrier approach, into an energy derivative plus finite size terms. The same has to be done with the functional derivative with respect to the potential appearing in the Feynman path-integral techniques.

Finite size effects can be very important in mesoscopic systems with real leads with several transmitting modes per current path. The energy appearing in the denominator of the finite size terms, Eqs. (25) and (31), corresponds in this case to the “longitudinal” energy of each mode, and so there is a divergence whenever a new channel is open. In the exact expressions there are no divergences; the problematic contributions of the finite size terms is cancelled out by the terms with energy derivatives.

GLOSSARY

ACKNOWLEDGMENT

M. O. would like to acknowledge the Spanish Dirección General de Investigación Científica y Técnica for financial support, Project Number BFM2000-1059.

REFERENCES

1. de Jongh, in “Nanophase Materials” (C. Hadjipanayis and R. Siegel, Eds.), p. 349. Kluwer Academic, Dordrecht, 1994.
2. G. Schmid (Ed.), “Clusters and Colloids.” VCH, Weinheim, 1994.
3. U. Simon and G. Schön, in “Handbook of Nanostructured Materials and Nanotechnology” (H. S. Nalwa, Ed.), Vol. 3, pp. 131–175. Academic Press, San Diego, 1999.
4. E. H. Hauge and J. A. Støvneng, *Rev. Mod. Phys.* 61, 917 (1989).
5. V. S. Olkhovsky and E. Recami, *Phys. Rep.* 214, 339 (1992).
6. C. R. Leavens and G. C. Aers, in “Scanning Tunnelling Microscopy III” (R. Wiesendanger and H. J. Güntherodt, Eds.), p. 105. Springer-Verlag, Berlin, 1993.
7. A. Enders and G. Nimtz, *Phys. Rev. B* 47, 9605 (1993).
8. A. Ranfagni, P. Fabeni, G. P. Pazzi, and D. Mugnai, *Phys. Rev. E* 48, 1453 (1993).
9. A. M. Steinberg, P. G. Kwiat, and R. Y. Chiao, *Phys. Rev. Lett.* 71, 708 (1993).
10. Ch. Spielman, R. Szipöcs, A. Stingl, and F. Krausz, *Phys. Rev. Lett.* 73, 708 (1994).
11. R. Landauer and Th. Martin, *Rev. Mod. Phys.* 66, 217 (1994).
12. Y.-P. Wang and D.-L. Zhang, *Phys. Rev. A* 52, 2597 (1995).
13. Y. V. Fyodorov and H.-J. Sommers, *J. Math. Phys.* 38, 1918 (1996).
14. R. Pelster, V. Gasparian, and G. Nimtz, *Phys. Rev. E* 55, 7645 (1997).
15. J. Ruiz, M. Ortuño, E. Cuevas, and V. Gasparian, *J. Phys. I France* 7, 653 (1997).
16. Ph. Balcou and L. Dutriaux, *Phys. Rev. Lett.* 78, 851 (1997).
17. G. L. Ingold and Y. V. Nazarov, in “Single Charge Tunnelling, Coulomb Blockade Phenomena in Nanostructures” (H. Grabert and M. Devoret, Eds.), p. 21. Plenum, New York, 1992).
18. L. Esaki, *Phys. Rev.* 109, 603 (1958).
19. T. E. Hartman, *J. Appl. Phys.* 33, 3427 (1962).
20. V. F. Rybachenko, *Sov. J. Nucl. Phys.* 5 (1967).
21. S. Bosanac, *Phys. Rev. A* 28, 577 (1983).

22. V. S. Olkhovski, E. Recami, F. Raciti, and A. K. Zaichenko, *J. Phys. I France* 5, 1351 (1995); A. M. Steinberg and R. Y. Chiao, *Phys. Rev. A* 49, 3283 (1994).
23. A. Enders and G. Nimtz, *J. Phys. I France* 2, 1693 (1992).
24. A. Enders and G. Nimtz, *Phys. Rev. E* 48, 632 (1993).
25. A. Enders and G. Nimtz, *J. Phys. I France* 3, 1089 (1993).
26. D. Mugnai, A. Ranfagni, R. Ruggeri, and A. Agresti, *Phys. Rev. E* 49, 1771 (1994).
27. A. Ranfagni, D. Mugnai, and A. Agresti, *Phys. Lett. A* 175, 334 (1993).
28. H. Grabert and M. H. Devoret, Eds., "Single Charge Tunnelling, Coulomb Blockade Phenomena in Nanostructures", p. 1. Plenum, New York, 1992.
29. D. V. Averin and K. K. Likharev, in "Single Charge Tunnelling, Coulomb Blockade Phenomena in Nanostructures" (H. Grabert and M. Devoret, Eds.), p. 311. Plenum, New York, 1992.
30. G. Schön and U. Simon, *Colloid Polym. Sci.* 273, 202 (1995).
31. J. G. A. Dubois, J. W. Gerristen, S. E. Shafranuk, E. J. G. Boon, G. Schmid, and H. Kempen, *Europhys. Lett.* 33, 279 (1996).
32. Mandelstam and Tamm, *Izv. Akad. Nauk SSSR* 9, 122 (1945).
33. D. I. Blokhintsev, "Grundlagen der Quantenmechanik," p. 388 Harri Deutsch, Frankfurt/Main, 1963.
34. I. A. Baz', *Sov. J. Nucl. Phys.* 4, 182 (1967).
35. I. A. Baz', *Sov. J. Nucl. Phys.* 5, 161 (1967).
36. M. Büttiker, *Phys. Rev. B* 27, 6178 (1983).
37. V. Gasparian, M. Ortuño, J. Ruiz, and E. Cuevas, *Phys. Rev. Lett.* 75, 2312 (1995).
38. R. Landauer, *Nature* 365, 692 (1993).
39. Th. Martin and R. Landauer, *Phys. Rev. A* 45, 2611 (1992).
40. E. Cuevas, V. Gasparian, M. Ortuño, and J. Ruiz, *Z. Phys. B* 100, 595 (1996).
41. Y. Japha and G. Kurizki, *Phys. Rev. A* 60, 1811 (1999).
42. M. Büttiker and R. Landauer, *Phys. Rev. Lett.* 49, 1739 (1982).
43. V. Gasparian and M. Pollak, *Phys. Rev. B* 47, 2038 (1993).
44. V. Gasparian, M. Ortuño, J. Ruiz, E. Cuevas, and M. Pollak, *Phys. Rev. B* 51, 6743 (1995).
45. A. G. Aronov, V. Gasparian, and U. Gummich, *J. Phys.: Condens. Matter* 3, 3023 (1991).
46. V. Gasparian, T. Christen, and M. Büttiker, *Phys. Rev. A* 54, 4022 (1996).
47. D. J. Thouless, *Phys. Rep.* 136, 94 (1974).
48. V. Gasparian, B. L. Altshuler, A. G. Aronov, and Z. H. Kasamian, *Phys. Lett. A* 132, 201 (1988).
49. C. R. Leavens and G. C. Aers, *Solid State Commun.* 67, 1135 (1988).
50. V. Gasparian, "Superlattices and Microstructures," to be published.
51. C. R. Leavens and G. C. Aers, *Solid State Commun.* 63, 1101 (1987); C. R. Leavens and G. C. Aers, in "Scanning Tunnelling Microscopy and Related Methods" (R. J. Behm, N. García, and H. Rohrer, Eds.), p. 59. Kluwer, Dordrecht, 1990.
52. V. Gasparian, M. Ortuño, J. Ruiz, and E. Cuevas, *Solid State Commun.* 97, 791 (1996).
53. G. García-Calderón and A. Rubio, *Solid State Commun.* 71, 237 (1989).
54. G. Iannaccone, *Phys. Rev. B* 51, 4727 (1995).
55. D. Sokolovski and L. M. Baskin, *Phys. Rev. A* 36, 4604 (1987).
56. J. A. Støvneng and E. H. Hauge, *Phys. Rev. B* 44, 1358 (1991).
57. R. P. Feynman and A. R. Hibbs, "Quantum Mechanics and Path Integrals." McGraw-Hill, New York, 1965.
58. M. Büttiker and R. Landauer, *Phys. Scr.* 32, 429 (1985).
59. M. Büttiker and R. Landauer, *IBM J. Res. Develop.* 30, 451 (1986).
60. Th. Martin and R. Landauer, *Phys. Rev. B* 47, 2023 (1993).
61. M. Büttiker, in "Electronic Properties of Multilayers and Low Dimensional Semiconductors" (L. E. J. M. Chamberlain and J. C. Portal, Eds.), p. 297. Plenum, New York, 1990.
62. M. Jonson, in "Quantum Transport in Semiconductors" (D. K. Ferry and C. Jacoboni, Eds.), p. 203. Plenum, New York, 1991.
63. L. D. Landau and E. M. Lifshitz, "Quantum Mechanics." Pergamon, New York, 1979.
64. A. P. Jauho and M. Jonson, *J. Phys.: Condens. Matter* 1, 9027 (1989).
65. Th. Martin, *Int. J. Mod. Phys. B* 10, 3747 (1996).
66. R. Landauer, *Ber. Bunsenges. Phys. Chem.* 95, 404 (1991).
67. A. P. Jauho, in "Hot Carriers in Semiconductor Nanostructures: Physics and Applications" (J. Shah, Ed.), p. 121. Academic Press, Boston, 1992.
68. D. Sokolovski and J. N. L. Connor, *Phys. Rev. A* 42, 6512 (1990).
69. H. A. Fertig, *Phys. Rev. Lett.* 65, 2321 (1990).
70. H. A. Fertig, *Phys. Rev. B* 47, 1346 (1993).
71. K. L. Jensen and F. Buot, *Appl. Phys. Lett.* 55, 669 (1989).
72. J. G. Muga, S. Brouard, and R. Sala, *Phys. Lett. A* 167, 24 (1992); S. Brouard, R. Sala, and J. G. Muga, *Europhys. Lett.* 22, 159 (1993); S. Brouard, R. Sala, and J. G. Muga, *Phys. Rev. A* 49, 4312 (1994).
73. N. Yamada, *Phys. Rev. Lett.* 82, 3350 (1999).
74. M. Gell-Mann and J. B. Hartle, in "Proceedings of the 3rd International Symposium on the Foundations of Quantum Mechanics in the Light of New Technology" (S. Kobayashi, H. Ezawa, Y. Murayama and S. Nomura, Eds.). Physical Society of Japan, Tokyo, 1990.
75. D. Sokolovski, *Phys. Rev. A* 66, 032107 (2002).
76. L. D. Landau and E. M. Lifshitz, "Electrodynamics of Continuous Media." Pergamon, New York, 1982.
77. F. Rana, S. Tiwary, and D. A. Buchanan, *Appl. Phys. Lett.* 69, 1104 (1996).
78. E. Martinet, E. Rosencher, F. Chevoir, J. Nagle, and P. Bois, *Phys. Rev. B* 44, 3157 (1991).
79. H. Z. Zheng, H. F. Li, Y. M. Zhang, Y. X. Li, X. Yang, P. Zhang, W. Zhang, and J. F. Tian, *Phys. Rev. B* 51, 11128 (1995).
80. J. Zinn-Justin, "Quantum Field Theory and Critical Phenomena." Oxford University Press, London, 2002.
81. J. A. Lopez Villanueva and V. Gasparian, *Phys. Lett. A* 260, 286 (1999).
82. J. Bardeen, *Phys. Rev. Lett.* 6, 57 (1961).
83. W. Pauli, "Handbuch der Physik" (S. Flugge, Ed.), Vol. V/1. Springer-Verlag, Berlin, 1926.
84. J. Leon, J. Julve, P. Pitanga, and F. J. de Urres, *Phys. Rev. D* 61, 062101 (2000).
85. J. Leon, *J. Phys. A* 30, 4791 (1997).
86. V. Gasparian, M. Ortuño, G. Schön and U. Simon, in "Handbook of Nanostructured Materials and Nanotechnology" (H. S. Nalwa, Ed.), p. 513. Academic Press, San Diego, 1999.
87. F. García-Moliner and J. Rubio, *J. Phys. C: Solid State Phys.* 2, 1789 (1969).
88. B. Velicky and I. Bartoš, *J. Phys. C: Solid State Phys.* 4, L104 (1971).
89. F. García-Moliner, *Ann. Phys.* 2, 179 (1977).
90. H. Ueba and S. G. Davison, *J. Phys. C: Solid State Phys.* 13, 1175 (1980).
91. E. Louis and M. Elices, *Phys. Rev. B* 12, 618 (1975).